

Review

Advances in Marine Self-Powered Vibration Sensor Based on Triboelectric Nanogenerator

Yongjiu Zou ^{1,2} , Minzheng Sun ¹, Weipeng Xu ¹, Xin Zhao ¹, Taili Du ^{1,2,*} , Peiting Sun ^{2,*}  and Minyi Xu ^{1,*} 

¹ Dalian Key Lab of Marine Micro/Nano Energy and Self-Powered Systems, Marine Engineering College, Dalian Maritime University, Dalian 116026, China

² Collaborative Innovation Research Institute of Autonomous Ship, Dalian Maritime University, Dalian 116026, China

* Correspondence: dutaili@dmlu.edu.cn (T.D.); sunptg@dmlu.edu.cn (P.S.); xuminyi@dmlu.edu.cn (M.X.)

Abstract: With the rapid development of advanced electronics/materials and manufacturing, marine vibration sensors have made great progress in the field of ship and ocean engineering, which could cater to the development trend of marine Internet of Things (IoT) and smart shipping. However, the use of conventional power supply models requires periodic recharging or replacement of batteries due to limited battery life, which greatly causes too much inconvenience and maintenance consumption, and may also pose a potential risk to the marine environment. By using the coupling effect of contact electrification and electrostatic induction, triboelectric nanogenerators (TENGs) were demonstrated to efficiently convert mechanical vibration movements into electrical signals for sensing the vibration amplitude, direction, frequency, velocity, and acceleration. In this article, according to the two working modes of harmonic vibration and non-harmonic vibration, the latest representative achievements of TENG-based vibration sensors for sensing mechanical vibration signals are comprehensively reviewed. This review not only covers the fundamental working mechanism, rational structural design, and analysis of practical application scenarios, but also investigates the characteristics of harmonic vibration and non-harmonic vibration. Finally, perspectives and challenges regarding TENG-based marine self-powered vibration sensors at present are discussed.

Keywords: triboelectric nanogenerators; energy conversion; self-powered vibration sensor; marine Internet of things



Citation: Zou, Y.; Sun, M.; Xu, W.; Zhao, X.; Du, T.; Sun, P.; Xu, M.

Advances in Marine Self-Powered Vibration Sensor Based on Triboelectric Nanogenerator. *J. Mar. Sci. Eng.* **2022**, *10*, 1348. <https://doi.org/10.3390/jmse10101348>

Academic Editor: Christos Tsabaris

Received: 1 August 2022

Accepted: 12 September 2022

Published: 22 September 2022

Publisher's Note: MDPI stays neutral with regard to jurisdictional claims in published maps and institutional affiliations.



Copyright: © 2022 by the authors. Licensee MDPI, Basel, Switzerland. This article is an open access article distributed under the terms and conditions of the Creative Commons Attribution (CC BY) license (<https://creativecommons.org/licenses/by/4.0/>).

1. Introduction

With the vigorous development of the Internet of Things technology, the sensor manufacturing technology and networking technology required in sensor networks have gradually developed and matured, making sensor networks widely used in many industrial and social fields [1–5]. Recently, with the development of information technology, artificial intelligence and big data, the marine transportation industry based on intelligent ships/smart shipping has become a new development trend [6–8]. Relying on smart ocean engineering, it is particularly important to accelerate the construction of marine stereo monitoring network while promoting the optimization and upgrading of marine industry and the development of intelligent ships [9,10]. As an information collection method with low cost and high degree of automation, sensor networks have been applied in the marine industry and a variety of marine activities, such as ship condition monitoring, marine environment monitoring, maritime security, and hydrological information collection [11–15]. Through continuous development in recent years, the application of sensor networks in the field of ship and ocean engineering has been continuously improved and achieved good results, and gradually become the main means of marine information collection.

The whole ocean sensor network is widely distributed in ships, ocean surface, underwater, offshore platforms and shore-based buildings, including displacement sensors,

velocity sensors, flow sensors, temperature sensors, pressure sensors, vibration sensors and tactile sensors [16–19]. The vibration sensor can sense the amplitude, frequency, velocity and acceleration of vibration to judge the working condition of mechanical equipment on the ship and the parameters of marine environment, which plays a very important role in the whole marine sensor network [20–22]. However, one of the main challenges facing the development of existing vibration sensors is the limited battery life of the traditional power supply mode, which requires periodic charging or battery replacement, and which greatly causes much inconvenience and maintenance consumption, especially in the case of a large number of distributed marine sensor networks [23–26]. Furthermore, most battery systems are built with toxic chemicals, which may pose potential marine environmental risks. Therefore, these vibration sensors urgently need sustainable, universal and environmentally energy solutions.

At present, the advanced vibration sensing technology commonly used in ships includes eddy current, electromagnetic, piezoelectric and triboelectric effect [27–31]. The eddy current vibration sensing technology has the advantages of simple structure, wide frequency range and strong anti-interference ability, but the surface cracks of the measured equipment and the conductivity and permeability of the material have an impact on the sensitivity [32–36]. An electromagnetic vibration sensor is mainly used to measure vibration velocity, which is less affected by ship temperature and humidity. Its structure is simple, but its structure size and weight are large, which is greatly affected by magnetic field. If the permanent magnet is used, the attenuation of the magnetic field will reduce its sensitivity [37–40]. The above two wired connection vibration monitoring systems have the disadvantages of high deployment cost, poor fault tolerance and maintainability, and lack of mobility flexibility [41–45]. Especially in some special and extreme cases, such as the vibration monitoring of equipment transmission parts in some sealing environment and mechanical rotation environment, it is difficult to realize the external power supply [46–49]. Piezoelectric vibration sensing technology has the advantages of high sensitivity, wide frequency range and self-powered supply, but it is greatly affected by the ambient temperature and humidity of the ship [50–56].

Recently, Wang's team invented the triboelectric nanogenerator (TENG) in 2012, which is a new energy conversion method based on Maxwell displacement current principle [57–60]. Combining the triboelectrification and electrostatic induction, the triboelectric nanogenerator can directly convert the mechanical movements with wide frequency distribution into electrical signals with high output voltage and high signal-to-noise ratio [61–68]. TENG has the advantages of low cost, light weight, simple structure, strong environmental compatibility and a wide range of material selection, and presents obvious advantages in the field of self-powered vibration sensing technology [69–78]. As a new research field, TENGs have achieved remarkable results in the application scenario of ship and ocean engineering [30,79–83]. It is used to convert marine mechanical vibration into reliable and obvious electrical signals to characterize the working condition of marine equipment or marine environmental parameters, which lays the foundation for the development of intelligent marine sensor network [84–89]. Some teams have been engaged in related research and have achieved some results. Wang's team of Beijing Institute of Nano-Energy and Systems has made great contributions to marine environmental monitoring based on TENG [90–93]. Xu's team of Dalian Maritime University has done some research on ship equipment condition monitoring based on vibration sensors [85,94–96]. Wu's team of China University of Geosciences has done extensive research on self-powered downhole TENG-based vibration sensors [97,98]. Specifically, the existing TENG-based marine self-powered vibration sensors can be mainly divided into harmonic vibration and non-harmonic vibration, and the specific classification is shown in Figure 1.

To provide a comprehensive and systematic review of marine self-powered vibration sensors based on TENG for the first time, the obvious advantages of TENGs in marine vibration monitoring are analyzed. Subsequently, the recent progress in practical marine applications of harmonic vibration sensors and non-harmonic vibration sensors is particularly

emphasized. In addition, the future development of marine self-powered vibration sensors based on TENG is prospected and challenged. This review will greatly accelerate the development of smart ocean and intelligent ship sensor networks, and have implications for providing ubiquitous and sustainable energy solutions for smart ocean sensor systems in the coming era of the marine Internet of Things.

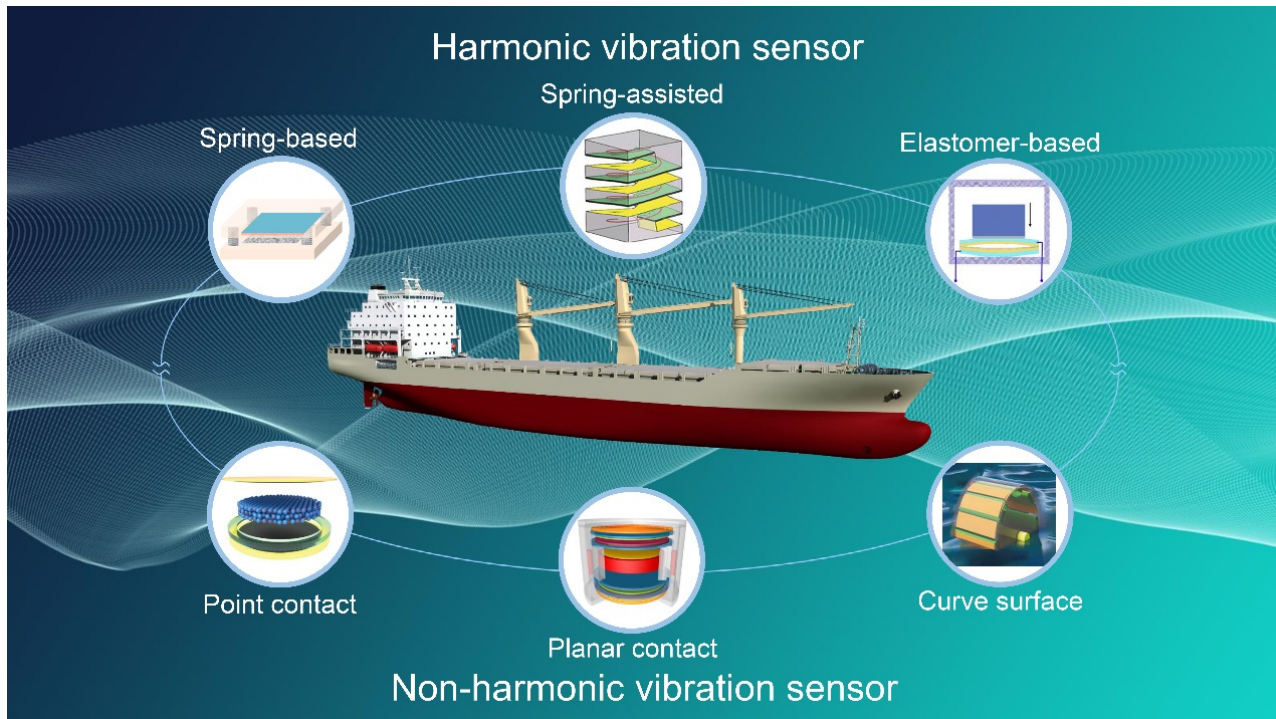


Figure 1. A marine self-powered vibration sensor based on a triboelectric nanogenerator.

2. TENG-Based Harmonic Vibration Sensor

When a vibration sensor is subjected to harmonic vibration, the physical force is proportional to the displacement and always points to the equilibrium position [99,100]. It is a periodic motion (such as spring oscillator motion) that is determined by the property of its own system. Recently, tremendous efforts have been made in developing harmonic vibration sensors based on TENG, which can use springs [90,93,98,101–103], elastomers [104–108] and spring-assisted structures [91,95,109,110] as core components to accompany the measured object to do regular reciprocating motion and realize the working condition monitoring of the vibration system through the electrical signals generated by them. If the harmonic vibration sensor is to be applied in the field of ship and ocean engineering, it is required to have unique structure design, stable working characteristics and high sensitivity. With this concern, this part makes statements according to the different core elastic components of the TENG-based harmonic vibration sensor.

2.1. Spring-Based Vibration Sensor

Spring-based vibration sensor uses spring as the core moving component, and spring is the most used core component of harmonic vibration. When the spring-based vibration sensor moves with the measured object, it mainly relies on the reciprocating action of the spring to cause alternating contact and separation of the triboelectric materials, thus generating electrical signals that can monitor the vibration state. To begin with, Zhao et al. reported a low-frequency self-powered triboelectric nano vibration accelerometer (TEVA) with high sensitivity, which provides a simple and cost-effective means for monitoring mechanical vibration [102]. The structure of TEVA is schemed in Figure 2a. The TEVA, with a multi-layered structure, is made up of polymethyl methacrylate (PMMA), Aluminum

(Al), and Kapton. The two PMMA substrates are connected by four springs installed at the corners of the substrates, leaving a narrow gap between the Aluminum and the Kapton, which are all modified with nanostructures. The working principle of the TEVA is shown in Figure 2b. The TEVA can achieve periodic contact and separation between two triboelectric layers at different speeds or accelerations to generate output signals. As shown in Figure 2c, the peak voltage increases almost linearly with the increase of acceleration when the frequency is 4 Hz and 6 Hz. The TEVA can measure mechanical vibration acceleration and provide guidance for marine equipment condition monitoring and fault diagnosis. Wang and Chen et al. also designed contact-separation TENGs in the form of four-corner spring supports to monitor vibration frequency [111,112]. In addition, some scholars have developed multiple sliding-mode TENGs to sense vibration signals using the tension of four springs [113–115].

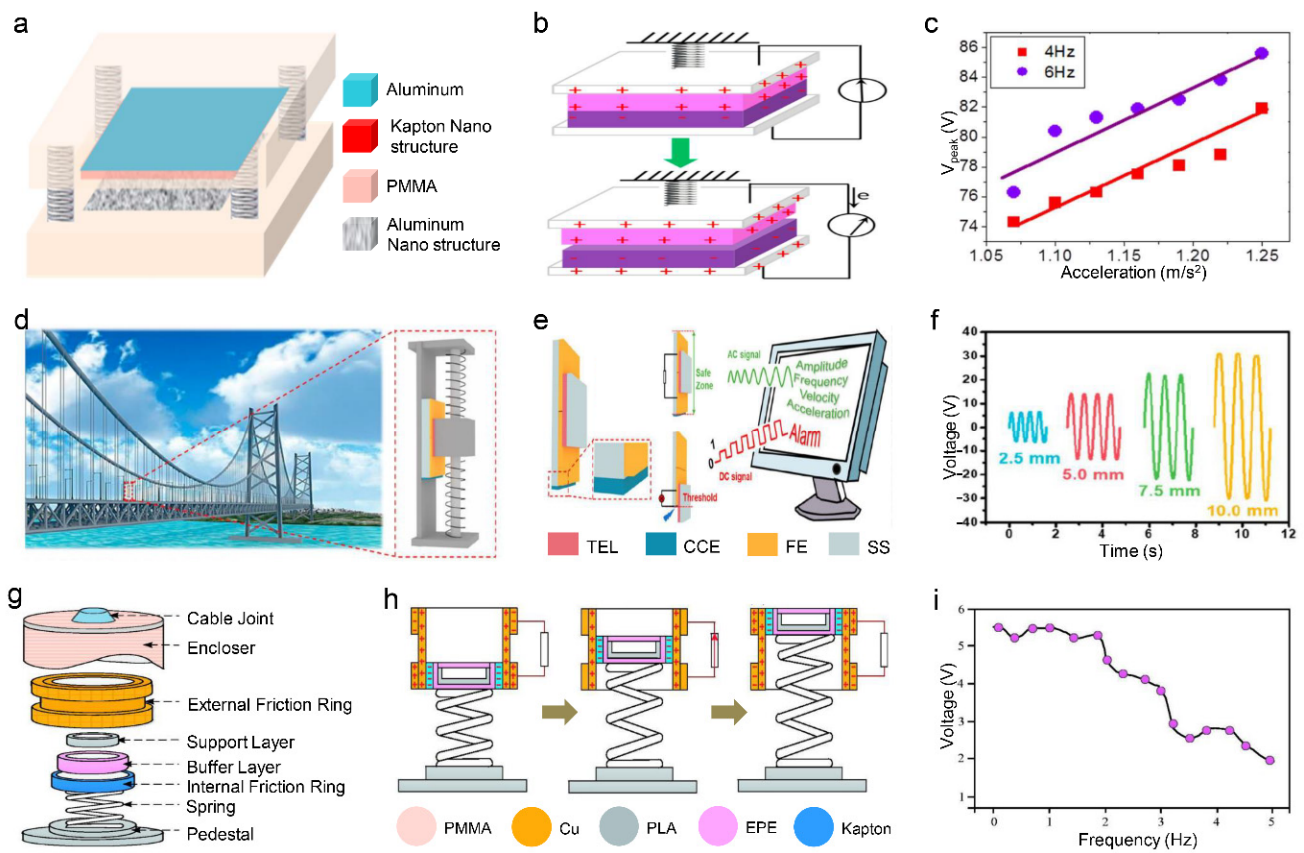


Figure 2. A spring-based vibration sensor: Part One. (a) Schematic illustration of the self-powered TEVA. (b) Working principle of the TEVA. (c) Relationship between peak voltage and acceleration when frequencies are 4 Hz and 6 Hz respectively. Reproduced with permission [102]. Copyright 2017, Elsevier. (d) Schematic structure of the AC/DC-TENG. (e) Working mechanism of the AC/DC-TENG. (f) Curve of AC/DC-TENG output voltage as a function of amplitude. Reproduced with permission [90]. Copyright 2020, American Chemical Society. (g) Schematic structure of the vibration sensor. (h) Schematic diagram of working process of the vibration sensor. (i) Dependence of the output voltage of the vibration sensor on the vibration frequency. Reproduced with permission [98]. Copyright 2020, SAGE Publications Ltd.

Using two springs, Li et al. developed a dual-mode triboelectric nanogenerator (AC/DC-TENG), which can realize real-time monitoring of vibration safety state without external power supply or software (Figure 2d) [90]. The structure of the AC/DC-TENG is made up of a slider and a stator, as shown in Figure 2e. The stator is composed of two friction electrodes (FEs), a charge collecting electrode (CCE), and an acrylic layer as a supporting substrate. Two FEs of equal size are pasted side by side on the supporting substrate,

with a gap of 0.5 mm, and a CCE is placed on the bottom edge of the supporting substrate. Fluorinated ethylene propylene (FEP) film is attached to the slider as a triboelectric layer. AC signals are generated when the slider slides reciprocally between the two FEs but does not exceed the edge of the acrylic substrate—that is, in the safe area. When a part of the slider moves in the danger zone, which is the part beyond supporting substrate, it will generate DC signal. Whether the vibration amplitude exceeds the vibration threshold can be judged by monitoring the change of signal type. As shown in Figure 2f, the V_{AC} of the AC/DC-TENG within the safety zone is well linearly proportional to the vibration amplitude, and so does the V_{DC} of the AC/DC-TENG within the safety zone. This AC/DC-TENG can continuously monitor the vibration amplitude and the health of the construction structure. Beyond that, a self-powered 3D acceleration sensor with a detection ranges from about 13.0 to 40.0 m/s^2 and a sensitivity of 0.289 $V \cdot s^2/m$ was proposed to characterize the acceleration in the axis direction in a mass-spring-damper mechanical system [116].

For TENGs with a single compressed spring, Wu et al. proposed a self-powered downhole vibration sensor based on a triboelectric nanogenerator [98]. As shown in Figure 2g, the vibrational sensor is mainly composed of an external friction ring, an internal friction ring, a buffer layer, a spring, and a pedestal, but the core components are the external friction ring and the internal friction ring. The internal friction ring is made by Kapton, and the external friction ring is made by Cu. The buffer layer made by expanding aple poly ephylene (EPE) is affixed to the inner wall of the internal friction ring, and the support layer made of polylactic acid (PLA) is stuck inside the buffer layer to keep the shape unchanged. The working principle of the sensor is shown in Figure 2h. Under the vibration excitation, the inner friction electric ring and the outer friction ring alternately contact and separate to make simple up and down harmonic motion, generating voltage and current pulse signals. As shown in Figure 2i, the output voltage decreases almost linearly with the vibration frequency from 1 Hz to 5 Hz. The output voltage signals are proportional to the vibration frequency. In addition, Seol et al. introduced an all-printed TENG (AP-TENG) working in sliding-mode [101]. As shown in Figure 3a, the AP-TENG is assembled from the structural framework of 3D printing and the functional contact layer of 2D printing. The 3D-printed part is composed of two springs, two cases, and the core oscillator. The two cases form a closed rectangular shell. The 2D-printed part consists of a PMMA layer with a grating pattern attached along the outer sidewall of the core oscillator and Ag electrode layer attached along the inner sidewall of the case. The working principle of the AP-TENG is shown in Figure 3b. The sliding contact and separation between the 2D-printed functional layers generate electrical signals. Figure 3c shows that the output open-circuit voltage increases linearly at different vibration speeds of 60 cm/s to 110 cm/s, which demonstrates that the AP-TENG can easily monitor the vibration speeds of the machinery. Wu et al. also employed a spring-based resonance coupling for sensing vibration frequency [117].

For TENGs with a single tensile spring, Hu et al. designed a suspended 3D spiral structure triboelectric nanogenerator (S-TENG) as a self-powered vibration sensor for monitoring vibration acceleration [93]. A schematic diagram of the S-TENG is shown in Figure 3d. The working parts that generate the signals are made up of two round plates, which are facing with each other. One is centered and fixed on the upper side of the cube. The other is pasted at the bottom of the spiral structure. The upper contact surface is an Al film as an electrode coated on anodic aluminum oxide (AAO) template. The lower contact surface is a Kapton film coated on the Cu electrode. Figure 3e depicts the working principle of the S-TENG. The alternating contact and separation between Al electrode and Kapton film can generate electrical signals as the spiral oscillates. Figure 3f shows the voltage signals at different accelerations. As the vibration acceleration increases, the measured voltage signal increases linearly. By integrating the S-TENG inside a buoy ball, wave fluctuation acceleration can be monitored through the generated output voltage signals, which shows great potential application value in marine science and environmental monitoring. In addition, Yuan et al. proposed a spring-oscillator based triboelectric nanogenerator (S-

TENG) to monitor the vibration frequency [118]. The basic structure of the S-TENG is depicted in Figure 3g. It is made up of the inner sidewall of the Poly tetra fluoroethylene (PTFE) tube and the nickel layer of the magnet which acts as both the positive triboelectric material and the sole electrode. Figure 3h illustrates the working principle of the single-electrode S-TENG. Driven by a steel spring, the magnet oscillates alternately up and down, and alternating sliding friction between the inside wall of PTFE tube and the magnet produces an output electric signal. Figure 3i shows the relationship between the output voltage and current of the S-TENG with the vibration frequency. When the frequency is bigger than 4 Hz, the output voltage and current both decrease with the increase of frequency and both of them maintain a good linear relationship.

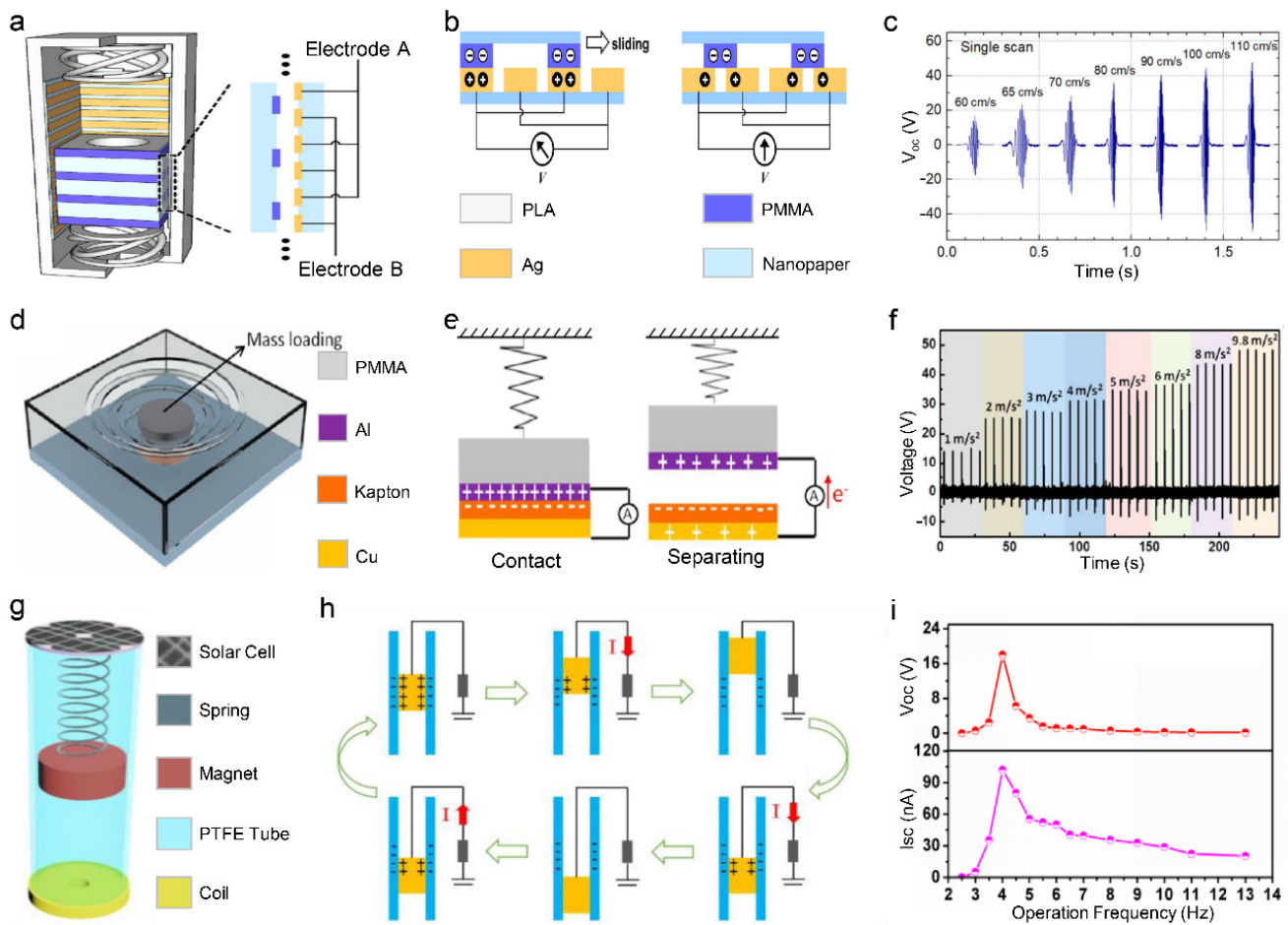


Figure 3. The spring-based vibration sensor: Part Two. (a) Structural design of the AP-TENG. (b) Working mechanism of the AP-TENG. (c) Output open-circuit voltage curve when the sliding velocity changes from 60 to 110 cm/s. Reproduced with permission [101]. Copyright 2017, Elsevier. (d) Schematic illustration of the S-TENG. (e) Working principle of the S-TENG. (f) Output voltage of the self-powered dynamic sensor when the acceleration changes from 1 to 9.8 m/s². Reproduced with permission [93]. Copyright 2013, American Chemical Society. (g) Schematic structure of the S-TENG. (h) Working mechanism of the S-TENG. (i) The V_{OC} and I_{SC} of the S-TENG at different operation frequencies. Reproduced with permission [118]. Copyright 2018, IOP Publishing Ltd.

2.2. Elastomer-Based Vibration Sensor

Elastomer-based vibration sensors mainly use elastomers as core components, such as elastic steel [105,119,120] and polymer elastic sheet [108,121–123]. Elastomers can directly or indirectly make triboelectric materials produce alternating contact and separation, resulting in electrical signals. Firstly, Wang et al. reported a sort of self-powered vibration sensor based on triboelectric nanogenerator (B-TENG), which presents the characteristics of

convenient production, remote monitoring, no energy consumption, high precision, large detection range [105]. The schematic structure of the B-TENG is shown in Figure 4a. The B-TENG was mainly composed of an Al (or Fe) plate and a PTFE film on a glass slide. The Al plate served as the contact electrode and contact surface and was connected to the vibration beam. A thin Au film was adhered onto the PTFE film as the back electrode. An Au-coated PTFE film was pasted onto a piece of glass slide to flatten the surface. The glass slide was fixed on a stationary stage. As depicted in Figure 4b, the working mechanism of the sensor is the periodic contact and separation between Al electrode and PTFE film to generate electrical signals. As shown in Figure 4c, the output voltage of the B-TENG increases almost linearly with the increase of the vibration amplitude. The vibration sensor possessed great potential in marine machinery operation monitoring, process control and safety applications in inaccessible environments. Similarly, the cantilever beam structural TENGs with one contact surface also uses polymer materials as elastic components [120,124].

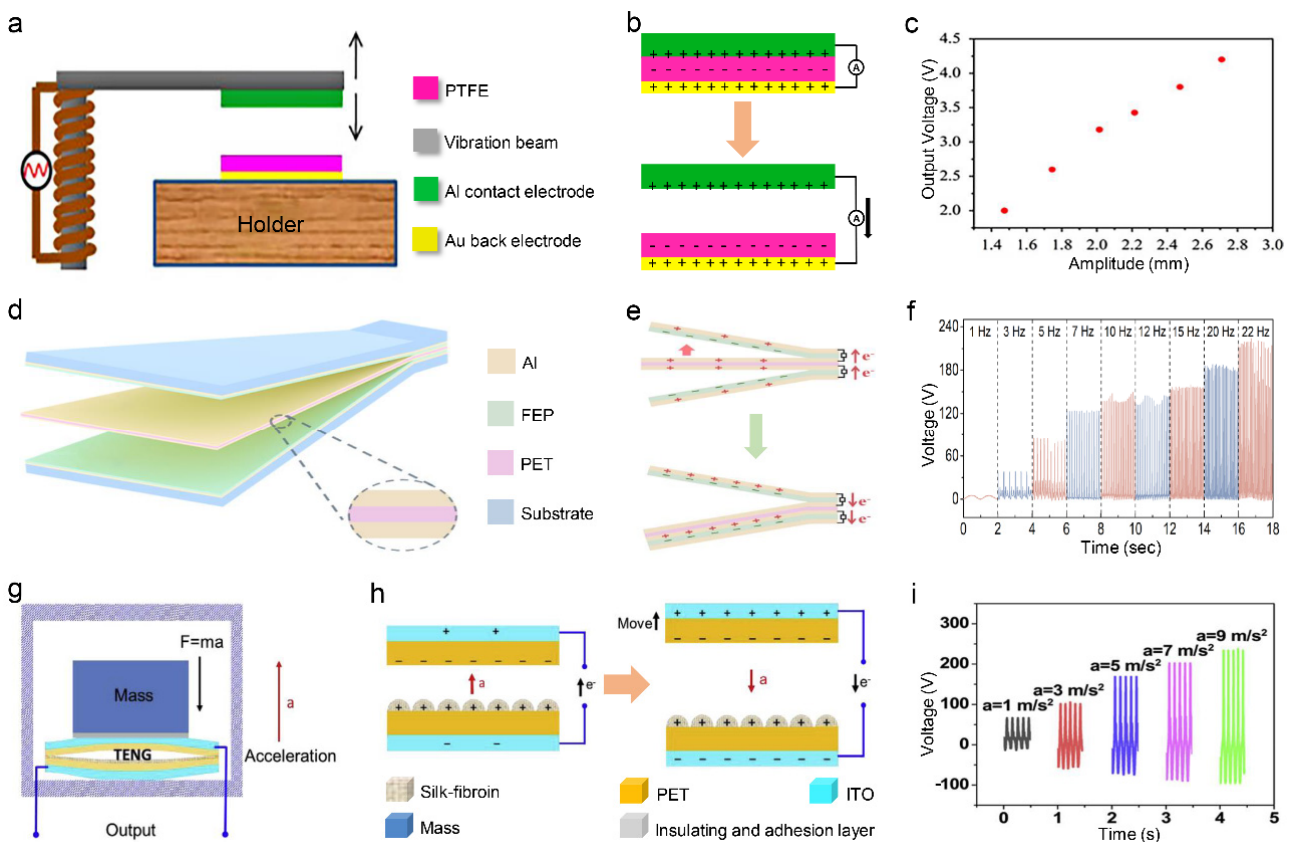


Figure 4. The elastomer-based vibration sensor. (a) Schematic structure of the B-TENG. (b) Working mechanism of the B-TENG. (c) Output voltage curve under different vibration amplitude. Reproduced with permission [105]. Copyright 2014, Elsevier. (d) Schematic structure and materials design of the C-TENG. (e) Working principle of the C-TENG. (f) Output voltage of the C-TENG when the frequency changes from 1 to 22 Hz. Reproduced with permission [121]. Copyright 2022, American Chemical Society. (g) Structure design of the self-powered acceleration sensor. (h) Working mechanism of the self-powered acceleration sensor. (i) Output voltage of the sensor when the acceleration changes from 1 to 9 m/s². Reproduced with permission [106]. Copyright 2019, Elsevier.

For the multi-layer cantilever structure, Ren et. al. firstly demonstrated a trapezoidal cantilever-structure triboelectric nanogenerator (C-TENG) that can monitor the low-frequency vibration [121]. As shown in Figure 4d, the C-TENG consists of two negative tribo-layers of FEP attached on two trapezoidal substrates and flexible Al electrodes attached on the Polyethylene terephthalate (PET) substrate sandwiched in the frameworks. The trapezoidal elastic film electrode is made into a cantilever structure, with the narrow

side of the trapezoidal fixed. The working principle of the C-TENG is demonstrated in Figure 4e. Under ambient vibration, the flexible vibration electrode moves between the upper and lower FEP triboelectric layers to generate electrical signals. Figure 4f depicts the output voltage signals of the C-TENG at frequencies from 3 to 15 Hz. The output voltage value also increases steadily with increasing frequency. The output voltage signals are well linearly proportional to the vibration frequency. The output voltage signals are well linearly proportional to the vibration frequency. Another triple-cantilever based TENG with the nanowire arrays fabricated onto the surfaces of beryllium–copper alloy foils show better output effect [123].

In addition, there are also multilayer structures using polymer elastic sheets. A self-powered and high sensitivity acceleration sensor based on triboelectric nanogenerator was reported by Wang et al. [106] The structure of the self-powered acceleration sensor is shown in Figure 4g. The sensor consists of a bottom shell, a TENG, an insulating layer, a mass, and a top shell. The triboelectric layers consist of silk–fibroin layer deposited on the PET layer and PET layer, which are all attached on the Indium Tin Oxides (ITO) electrodes. The TENG with an arch-shape supports the mass. The working principle of the sensor is schematically shown in Figure 4h. The output voltage signals of the sensor are generated by the contact-separation motion between the triboelectric layers of the TENG. The acceleration sensor is fixed on the top platform of the shaker, which supplies a vibration excitation with adjustable acceleration. As shown in Figure 4i, the open-circuit voltage has been measured under different vibration acceleration from 1 m/s^2 to 9 m/s^2 . The output voltage of the sensor increases linearly with the increase of vibration accelerations. This acceleration sensor has potential application value in some vibration monitoring systems and provides better guidance for the development of self-powered sensors. Li and Wang et al. also used the structure of multilayer polymer elastic plates to perceive vibration signals [108,125]. Beyond that, the sponge and a porous all-carbon material that is like a real metallic spring are also innovatively used as the elastomer to design the TENG [107,126].

2.3. Spring-Assisted Vibration Sensor

The spring-assisted vibration sensor adopts the spring-assisted structure as the core component, mainly including the combination of spring and polymer bullet and the combination of spring and silica gel. Firstly, Tian et al. proposed a kind of spherical TENG (S-TENG) with spring-assisted multilayered structure working in a contact-separation mode [91]. The S-TENG can monitor the amplitude of water fluctuation. The schematic structure of the S-TENG is shown in Figure 5a. The S-TENG is mainly composed of a thick Kapton film shaped to a zigzag structure deformed at evenly spaced intervals, serving as the substrate, and a spherical multilayered TENG with spring assistance. The S-TENG has five TENG units. Each unit is made up of Al foil and FEP film as the effective triboelectric layers. The working principle of each TENG unit is demonstrated in Figure 5b. The alternating contact and separation between the Al electrode and FEP film generate electrical signals. Figure 5c illustrates the output voltage of the S-TENG under different output voltage amplitudes of the function generator, which can simulate the different amplitudes of wave fluctuation. When the water fluctuation amplitude increases from 1.2 to 2.5 V, the electrical signal increases linearly. The S-TENG could monitor wave fluctuation amplitude employing the generated output voltage signals, which is a giant leap toward the dream of combining blue energy with self-powered vibration sensors compared with previous studies.

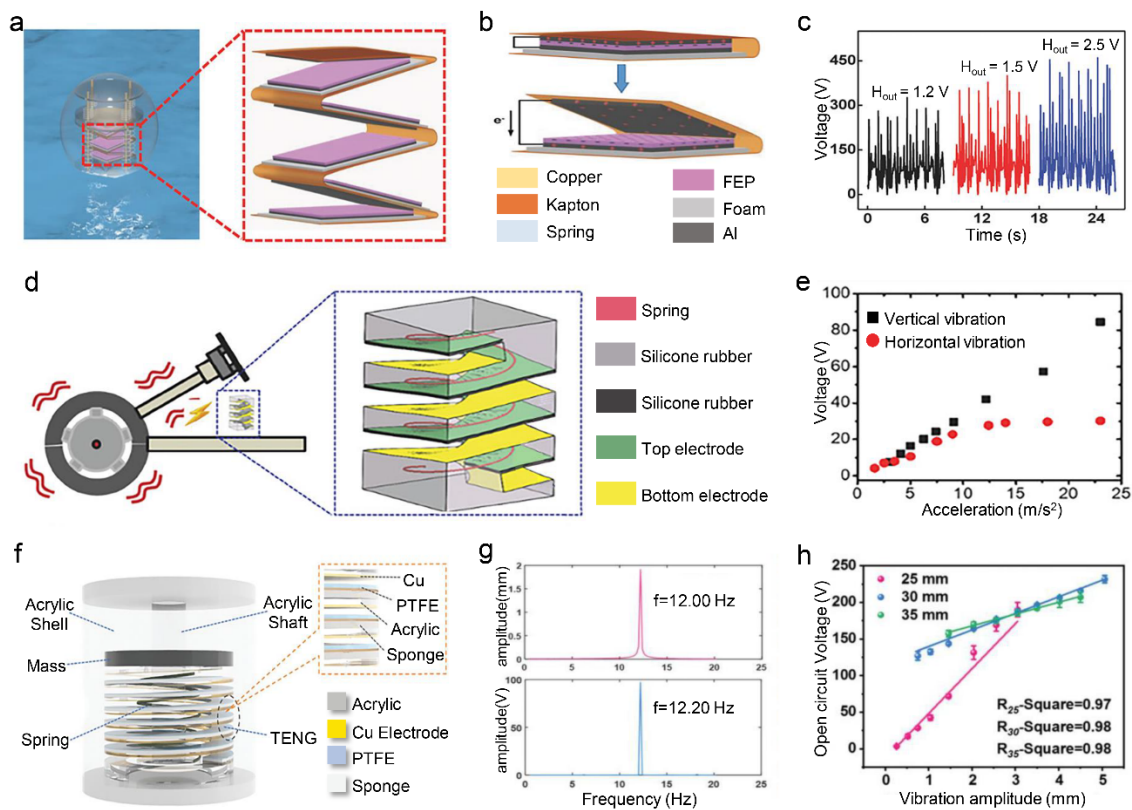


Figure 5. The spring-assisted vibration sensor. (a) Schematic diagram of a spring-assisted spherical TENG floating on water. (b) Working mechanism of each TENG unit of spherical TENG. (c) Relationship between output voltage and external excitations. Reproduced with permission [91]. Copyright 2018, Wiley-VCH. (d) Schematic structure of the spring-based TENG. (e) Relationship between output voltage and acceleration of S-TENG under vertical and horizontal vibration excitation. Reproduced with permission [95]. Copyright 2017, Wiley-VCH. (f) Schematic illustration of the spring-mass based TENG. (g) Vibration amplitude signal of the spring-mass based TENG at different frequency. (h) Relationship between voltage signal and vibration amplitude. Reproduced with permission [109]. Copyright 2022, Wiley-VCH.

In addition to the above multi-layer structures, spiral structures are more widely used. Xu et al. first designed a TENG integrated with elastomer and spring (S-TENG) to form a helical structure along a spring wire [95]. The spring-based TENG can be used to sense the acceleration and frequency of vibration as a self-powered vibration sensor. As illustrated in Figure 5d, the S-TENG is made up of spring, silicone rubber, and a conductive elastomer electrode. The elastomeric electrode consists of well-mixed silicone rubber and carbon nanofiber. Along the cut surface of the elastomer-spring helical structure, a layer of conductive electrode is placed at the lower surface of the helical structure covered by a layer of silicon rubber, and another layer of electrode is placed at the top surface of the helical structure. The periodic contact and separation between the silicone rubber and the top electrode can generate electrical signals. As shown in Figure 5e, the output voltage signal increases with the increase of vertical vibration acceleration, and the S-TENG is proper to measure vertical vibration acceleration in the range of 0 m/s² to 25 m/s². Under vertical vibration excitation, the surface of the tribo-materials can achieve full contact, but only partial contact under horizontal vibration excitation. Under the vertical vibration excitation, the output voltage of S-TENG is larger, and the linear regression coefficient of determination (R^2) is 0.9938, which shows a good linear relationship between the output voltage and the amplitude. Therefore, it should be used as a vertical vibration sensor to better exploit its sensitivity advantage. As a self-powered vibration sensor, the newly designed S-TENG has great potential in monitoring the working condition of the machinery on ships. In addition,

another spring-mass based helical TENG (S-TENG) was developed for online vibration monitoring, which presents superior sensing capability and measurement accuracy [109]. As illustrated in Figure 5f, the S-TENG employed the spring-mass as the framework with a six-layered helical structure. The Cu foils are attached to the upper and lower surfaces of the helical layer as the electrodes, and the PTFE film is covered on the surface of the bottom Cu electrodes to act as the triboelectric layers with the top Cu electrodes. With the external vibration excitation, the alternating contact and separation of the PTFE film and top Cu electrode generate electrical signals. Meanwhile, the vibration frequency can be obtained by fast Fourier transform of output voltage, and the calculated frequency corresponds to that of the laser sensor in Figure 5g. As shown in Figure 5h, the S-TENG was designed into different overall vibration spaces of 25, 30 and 35 mm. In different vibration spaces, the V_{oc} increases linearly with the vibration amplitude in the low amplitude area (0.2~3 mm). Therefore, the S-TENG could monitor the vibration amplitude. This feedback signal proves the excellent sensing capability of the S-TENG as a vibration amplitude detection sensor. In addition, a self-powered wireless acceleration sensor monitoring system is developed using a similar spiral structure as above to measure the acceleration signal of the vibration source [110].

In conclusion, applying the TENG-based harmonic vibration sensor to monitor vibration signals has made excellent progress in the field of ship and ocean engineering. To achieve long-term tracking of the condition of ship equipment and marine environment, these harmonic vibration sensors based on TENG should be robust and durable. In addition, reliable sensitivity is also very important for harmonic vibration sensors to perceive vibration signals. The harmonic vibration sensor mainly relies on the deformation of spring or spring assisted structure to sense the external vibration excitation, and the elasticity and stiffness of the core elastic body have a relatively large impact on the output signal. Further research opportunities lie in the selection of springs or other elastomers with appropriate elasticity and stiffness for application objectives and scenarios, based on the reasonable structure design.

3. TENG-Based Non-Harmonic Vibration Sensor

When the vibration sensor is subjected to the non-harmonic vibration, it also does reciprocate motion on both sides of the equilibrium position but does not follow the sinusoidal vibration. The moving parts in TENG are no longer limited by spring and elastic stiffness and can be forced to vibrate with the measured object freely. This may lead to the output signal of TENG not being synchronized with the vibration of the measured object, but it can be unified through the later data processing. When TENG is in vibration motion, the internal motion mechanism as one of the triboelectric materials will alternately contact and separate with another triboelectric material in the process of motion, and the contact form can be a point contact, plane contact and curve surface contact. According to the different contact forms of the two triboelectric materials, the TENG-based non-harmonic vibration sensors are described respectively below.

3.1. Point Contact Vibration Sensor

The point contact vibration sensor refers to two kinds of triboelectric materials that are contacted to generate electricity in the form of points. Generally, one of the triboelectric materials uses powder or particles, and the number is relatively large. Although the power generation in this way is not high and the output signal is relatively weak, it is more suitable as a sensing signal. To begin with, Liu et al. proposed a high-frequency vibration sensor (HVS) with layer-powder-layer structure, presenting excellent vibration perception ability [127]. Figure 6a shows the structure of HVS. The HVS is composed of two round graphite-coated alumina ceramic sheets, the mixed powder of PTFE and Ag, and an acrylic gasket. The working principle of HVS is shown in Figure 6b. Under external stimulation, the alternative contact and separation between the mixed powder and the graphite electrodes generate electrical signals. The HVS shows a wide frequency

response range of 3–133 kHz. Figure 6c demonstrated that the output voltage signal of HVS decreases with the increase of the distance from the vibration source to the HVS. HVS has also been demonstrated in engine vibration monitoring. The voltage signal of the HVS is basically 0 when it is not started and gets larger when it is started (Figure 6d). The facile and effective vibration monitoring system based on the HVS can provide a platform for various vibration monitoring scenarios. The self-powered high-frequency vibration sensor is an ideal choice for a next-generation vibration sensor.

In addition, Lu et al. reported a biocompatible sugar based triboelectric nanogenerator (S-TENG) with outstanding vibration sensing ability [128]. Figure 6e shows the structure of the S-TENG, which is made up of sugar particles and two hemispherical spherical shells with conductive metal layers on the inner surface as conductive layers. Figure 6f depicts the working principle of the S-TENG. Under the stimulation of external vibration, sugar particles alternately contact and separate with the conductive layers back and forth, and thus generate the electrical signals. The S-TENG is capable of monitoring vibration in multiple directions. As shown in Figure 6g, the open-circuit voltage of the S-TENG increases with the increase of vibration frequency under the same vibration angle. When the vibration direction is perpendicular to the two electrodes, the voltage is the highest, but the curve is the steepest, and the frequency can be perceived more accurately. It is worth mentioning that even if the vibration direction is parallel to the two electrodes, the voltage can reach 58.1V at the vibration frequency of 4 Hz, which is an obvious electrical signal output, making it of great value in vibration monitoring.

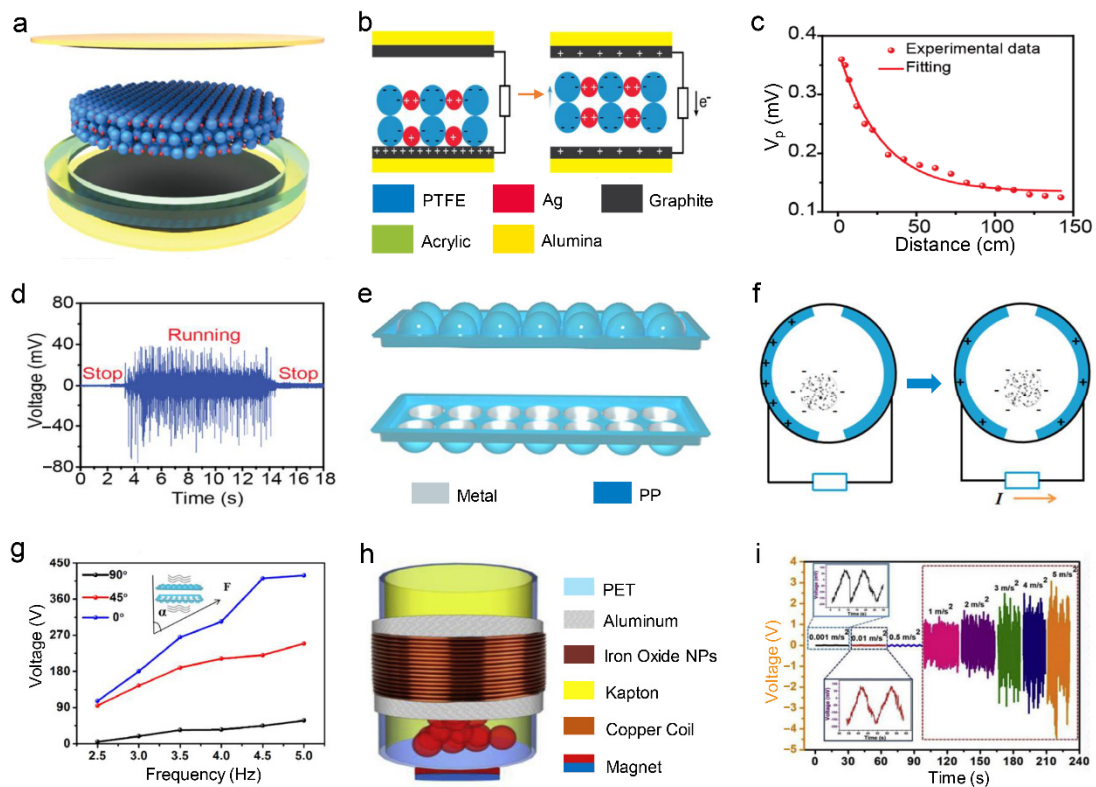


Figure 6. The point contact vibration sensor. (a) Structural design of the HVS. (b) Schematic showing the full cycle of the electricity generation process of the HVS. (c) Attenuation results with increased distance. (d) The output voltage waveform of HVS after the engine starts and stops. Reproduced with permission [127]. Copyright 2021, Elsevier. (e) Structural design of the S-TENG. (f) Schematic diagram of the working principle of the S-TENG. (g) The open-circuit voltage working at different vibration angles. Reproduced with permission [128]. Copyright 2021, Elsevier. (h) Schematic structure of the MP-HG. (i) The relation curve between electrical signal output of MP-HG device and different acceleration. Reproduced with permission [129]. Copyright 2019, Elsevier.

In addition, iron oxide nanoparticles are widely used in point contact TENG, especially in combination with electromagnetic induction. Vivekananthan et al. developed a magnetic nanoparticle derived cylindrical hybrid generator (MP-HG) with full packed structure, which can not only monitor the working condition of the marine equipment such as compressors but also can be used to warn people against possible natural disasters caused by waves [129]. MP-HG works on the free-standing mode. Figure 6h demonstrates the structure of MP-HG. It consists of a cylindrical PET, a rolled Kapton film, Cu wires, Al electrodes and Fe₂O₃ particles. Kapton film acts as the negative triboelectric layer while Fe₂O₃ particles act as positive triboelectric material. When subjected to external vibrations, Fe₂O₃ particles move upward and down, and alternately contact and separate with the upper and lower Kapton film, thus generating electrical signals. To demonstrate the application value of the MP-HG, we applied it to the vibration monitoring of the marine air compressor. Figure 6i shows the voltage output under different vibration accelerations. When the vibration acceleration is less than 1 m/s², the output voltage signal is basically 0, and the voltage increases with the increase of vibration acceleration when the vibration acceleration reaches 1 m/s². The MP-HG may pave the way for the practical application of self-powered vibration sensors in the future. A surface functionalized ferric oxide nanoparticle, which has strong ferromagnetism and high triboelectricity, shows better output effect [130]. In addition, Lai et al. adopted nanoporous SiO₂ particles for detecting vibrations and movement, which has a great potential in the underwater environment monitoring [131].

3.2. Planar Contact Vibration Sensor

Planar contact vibration sensor refers to the contact electricity generation of two triboelectric materials in the form of plane, and the electrical signal generated in this way is more obvious than that of point contact. Among them, the planar contact vibration sensor with axial motion of internal moving parts is the most common [96,97,132–134]. Firstly, Zhang et al. proposed a magnetically levitated triboelectric nanogenerator (ML-TENG) with the characteristics of high efficiency, advanced sensitivity and good stability [135]. The ML-TENG is composed of two TENGs and one electro-magnetic generator (Figure 7a). The TENG is made up of a one-piece membrane structure formed of polyamide, Al electrode, silicone and PET. PET serves as the support layer and the substrate layer. The working mechanism of the TENG is shown in Figure 7b. When external amplitude is greater than 5 mm, the arc gel pad moves upward and down, causing the nylon microfiltration membrane to alternately contact and separate from the silicone membrane, thus generating electrical signals. The sensitivity of the TENG is so high that even slight vibrations caused by flapping can be monitored when the ball lands. There is also a good correlation between TENG's output current and vibration acceleration. As shown in Figure 7c, the short-circuit current of TENG is from 50 nA to 1.1 μA when the acceleration is from 2 m/s² to 30 m/s² with the vibration amplitude of 7.5 mm. This work not only provides a new approach to the field of mechanical vibration perception, but also represents a solid step forward in the development of self-powered monitoring technology. Using the same axially moving contact-separation mode, another triboelectric accelerometer shows good linearity with a sensitivity of 15 V/g in 0–1.5 g with an optimized gap of 1.5 mm [133]. In addition, The V-TENG working in axial sliding mode, can synchronously measure the drill string vibration frequency and amplitude, which is more suitable for downhole conditions [97]. In addition to the above axial motion, the rotating motion of the core component can also directly sense the vibration signal [136,137].

In addition to the axial and rotational motion above, the non-directional motion of the core component can also be used to sense vibration information [138–141]. Du et al. proposed a robust silicone rubber strip-based triboelectric nanogenerator (SRS-TENG), which has the advantages of strong robustness, high stability, and broadband vibration range [142]. As shown in Figure 7d, the SRS-TENG can be used as a universal vibration sensing device in a variety of applications including ships and hydroelectric power plants.

The SRS-TENG is composed of two conductive aluminum electrodes supported by the PLA and a silicone rubber strip in the rectangular prism. Figure 7e shows the working principle of the SRS-TENG. Under the external vibration excitation, the periodic contact and separation between the silicone rubber strip and the aluminum electrodes generate electrical signals. Figure 7f demonstrated that the output short-circuit current of the SRS-TENG increases linearly with the increase of the vibration amplitude. Therefore, the SRS-TENG has potential applications in self-powered vibration sensing in the field of ships and oceans. Beyond that, Xia et al. developed a multiple-frequency high-elasticity triboelectric nanogenerator based on the water balloon (WB-TENG), which can monitor slight wave vibration [143]. The WB-TENG consists of two parts, a square box, and a water balloon (Figure 7g). The square box is composed of six identical acrylic substrates, covered with conductive copper foil tape and a nylon film. The water balloon includes PVC film and the sodium chloride solution. A conductive copper wire is inserted into the sodium chloride solution. Figure 7h demonstrates the working principle of WB-TENG. When the balloon swings close to or away from the nylon surface, the external circuit will produce opposite current signals. During the continuous swing of the water balloon inside the box, WB-TENG can continuously generate alternating current signals. Due to its sensitive response to external mechanical vibration, WB-TENG can also be employed to measure wave height. As shown in Figure 7i, the output voltage has an obvious linear relationship with wave height, and the output voltage increases from 46 V to 213 V when the wave height increases from 0.5 cm to 3.0 cm. The unique operating mechanism makes it a potentially new application for vibration monitoring in the marine field.

3.3. Curved Surface Contact Vibration Sensor

Curved surface contact vibration sensor refers to the contact electricity generation of two triboelectric materials in the form of curved surface. In this way, the contact area is the largest, and the generated electrical signal is the most obvious, so it is also the most widely used. Many scholars have done a lot of research on the curved surface contact mode, and the spherical contact structure is the most widely studied because it is easier to design and process [144–146]. Firstly, Zhang et al. reported a spherical three-dimensional triboelectric nanogenerator (3D-TENG) with a single electrode, which can monitor signals uniformly and stably, promoting the development of self-powered sensor systems [92]. The structure of the 3D-TENG is illustrated in Figure 8a and is composed of two spheres and a thin Al foil. One of the spheres is a Polyfluoroalkoxy (PFA) ball formed by an etched PFA film on an ordinary rubber ball, the other sphere is a transparent shell. The Al foil is attached to the inner surface of the outer sphere. Under the stimulation of external vibration, the PFA ball moves upward and down, alternately contacting and separating with the Al electrode, and thus generates periodic electrical signals. The 3D-TENG is utilized as a self-powered acceleration sensor with detection sensitivity of 15.56 V/g. As shown in Figure 8b, the apparent linear relationship between output voltage and vibration acceleration is revealed by fitting the data. As the vibration acceleration increases from 1.01 g to 1.99 g, the output voltage increases linearly from 4.5 V to 30.8 V. The output voltage of 3D-TENG is uniform and stable, which is beneficial to the practical application of the sensor. The 3D-TENG can monitor vibration effectively and opens many potential applications in self-powered vibration sensor systems. Using a similar structure, Wu et al. proposed a spherical TENG with a measurement range of 0–8 Hz and a test error of less than 2% [147]. In addition, Xiao et al. proposed a honeycomb structure inspired triboelectric nanogenerator (HSI-TENG), which can work in any vibration frequency and direction and monitor the starting state of marine diesel engine (Figure 8c) [94]. The structure of the HSI-TENG is shown in Figure 8d and is composed of two copper electrode layers with sponge bases and one honeycomb frame. The honeycomb frame with PTFE ball is fixed between two parallel copper electrode layers and encapsulated on two acrylic plates. The sponge bases are filled between the copper films and the acrylic plates. Figure 8e demonstrates the working principle of the HSI-TENG. When HSI-TENG is subjected to external vibration, the PTFE

ball moves upward and down, and alternately contacts and separates with the upper and bottom copper film, thus generating the electrical signals. When the HSI-TENG is installed on a diesel engine (Figure 8e), the output current of HSI-TENG can be obtained as the diesel engine starts and stops (Figure 8f). The short-circuit current can get to 2 μA during normal operation of the diesel engine, proving that the HSI-TENG can be used as an active self-powered sensor to monitor the engine working condition effectively. The excellent performance of HSI-TENG makes it have great potential in mechanical monitoring and provides a novel strategy for self-powered machinery monitoring. Similarly, Du et al. also demonstrated the bouncing-ball triboelectric sensor (BB-TENG) with a high signal-to-noise ratio of 34.5 dB at the vibration frequency of 10 Hz to 50 Hz by using the same structure of single ball forced vibration [85,148].

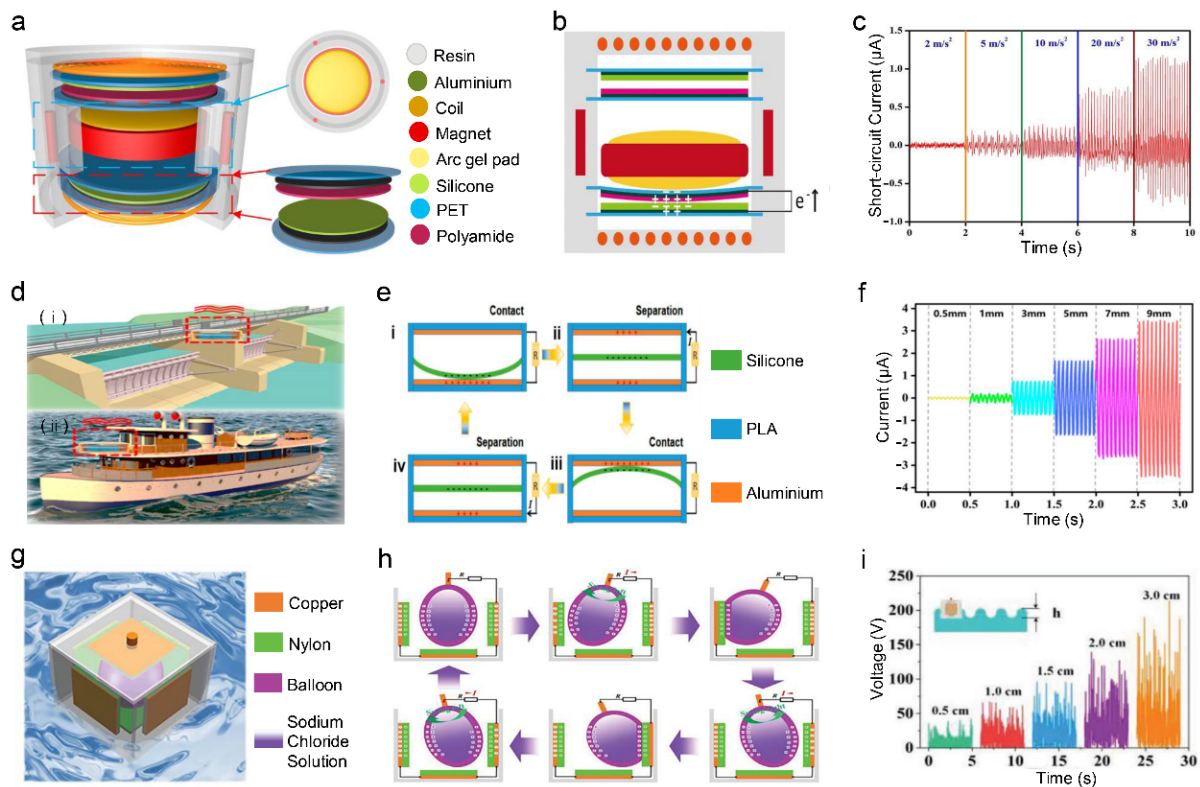


Figure 7. A planar contact vibration sensor. (a) Structural diagram of hybrid generator. (b) Schematic diagram of electricity generation process with amplitude greater than 5 mm. (c) Short-circuit current of the TENG at different accelerations. Reproduced with permission [135]. Copyright 2017, Elsevier. (d) Application scenarios of the SRS-TENG. (e) Schematic showing the full cycle of the electricity generation process of the SRS-TENG. (f) The relation between short-circuit current of SRS-TENG and different vibration amplitude. Reproduced with permission [142]. Copyright 2022, MDPI. (g) Schematic structure of the WB-TENG floating on the sea. (h) Schematic diagram of the electricity generation process of the WB-TENG. (i) Output voltage of WB-TENG at different wave vibration heights. Reproduced with permission [143]. Copyright 2020, Wiley-VCH.

For an aspheric contact vibration sensor, Zhao et al. proposed tumbler-shaped hybrid triboelectric nanogenerators (TH-TENG), which is composed of an external liquid TENG and an internal rolling-ball TENG [149]. The TH-TENG has characteristics of high novel structure, high efficiency, and good stability. Figure 8g shows the structure of TH-TENG, it is composed of a conical shape of the upper three-layer film and a hemispherical shape of the lower five-layer structure. The application scenario is explored as shown in Figure 8h. The working principle is shown in Figure 8i. When waves flow randomly, TH-TENG makes alternating tilting motions, and the outer wall alternately contacts and separates from the water surface, generating a current signal. The output performance of TH-TENG varies with

wave height as shown in Figure 8j. The output current increases from 0.2 μA to 0.6 μA as the wave height increases from 6 cm to 18 cm. TH-TENG can monitor wave vibration height and wave frequency simultaneously in an amphibious environment. Besides, Rui et al. reported a high-performance cylindrical pendulum shaped triboelectric nanogenerator (CP-TENG) with innovative arched film structure, possessing the advantages of large contact area, small friction, and multi-direction vibration signal monitoring [150]. Figure 9a depicts the construction of the CP-TENG, which includes an internal rotor, an external stator, two bearings in the center and a mass block with arched FEP films on the inner wall. The stator and rotor are mostly made of acrylic cylinder, with two caps on each end. There are several Al electrodes in the stator and many arched FEP films in the rotor. The working mechanism of CP-TENG is shown in Figure 9b. Under the external vibration, the mass with arched FEP film swings back and forth to the left and right, and the arched FEP film alternately contacts and separates with electrode-I and electrode-II, thus generating electrical signals. Figure 9c shows that the I_{sc} of the CP-TENG decreases gradually with θ from 0° to 90° . The θ is defined as the angle between the vertical motion of the wave and the axial direction of the CP-TENG. Figure 9d demonstrates the outstanding performance of CP-TENG for vibration direction sensing.

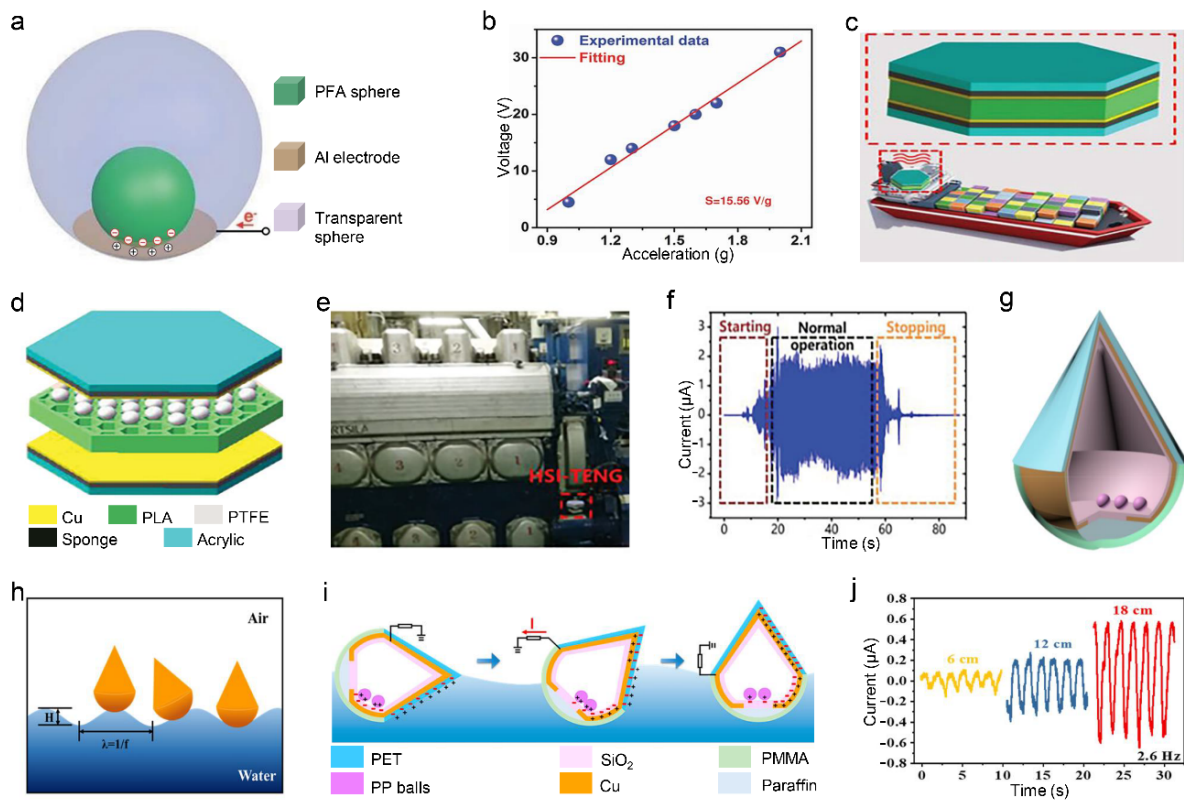


Figure 8. A curved surface contact vibration sensor: Part One. (a) Structure design of the 3D-TENG. (b) Relationship between the output voltage and acceleration. Reproduced with permission [92]. Copyright 2014, Wiley-VCH. (c) Schematic illustration of the HSI-TENG for vibration sensing. (d) Schematic structure of the HSI-TENG. (e) Photograph of HSI-TENG used for monitoring the working condition of the diesel engine on the ship. (f) The output short-circuit current of HSI-TENG after the diesel engine starts and stops. Reproduced with permission [94]. Copyright 2019, Wiley-VCH. (g) Schematic illustration of the TH-TENG unit. (h) A schematic of movement on the sea. (i) Working mechanism of the TH-TENG from tilt to neutral in the sea. (j) Output current at different wave vibration heights. Reproduced with permission [149]. Copyright 2020, Elsevier.

More distinctively, Zhang et al. proposed a self-powered acceleration sensor based on liquid metal(LM-TENG) with the advantages of high sensitivity and stability [151]. Figure 9e demonstrates the structure of the LM-TENG, which consists of an inner Hg

droplet and an outer acrylic. The acrylic surface has a thin copper film and a layer of Cu-coated Poly (vinylidene fluoride) (PVDF). Besides, the acceleration sensor can be fixed on the air compressor to monitor vibration condition (Figure 9f). The working principle of LM-TENG is shown in Figure 9g. When the acceleration sensor is subjected to external vibration, the mercury droplet moves upward and down, resulting in the electrical potential imbalance, thus producing electrical signals. Figure 9h shows the relationship between the output signal of the acceleration sensor and the start-stop state of the air compressor. As the air compressor started, the open circuit voltage quickly rose to 0.6 V and then slowly rose to 0.75 V until it stopped, which illustrates the sensitivity of the LM-TENG. The LM-TENG can measure the vibration of mechanical equipment in real time and has potential application prospect in vibration monitoring and troubleshooting of ship equipment. In addition, Deng et al. also developed a liquid-metal-based freestanding triboelectric generator (LM-FTENG) for vibration sensing, which provides an effective method for low-frequency and multidirectional vibration sensing [152].

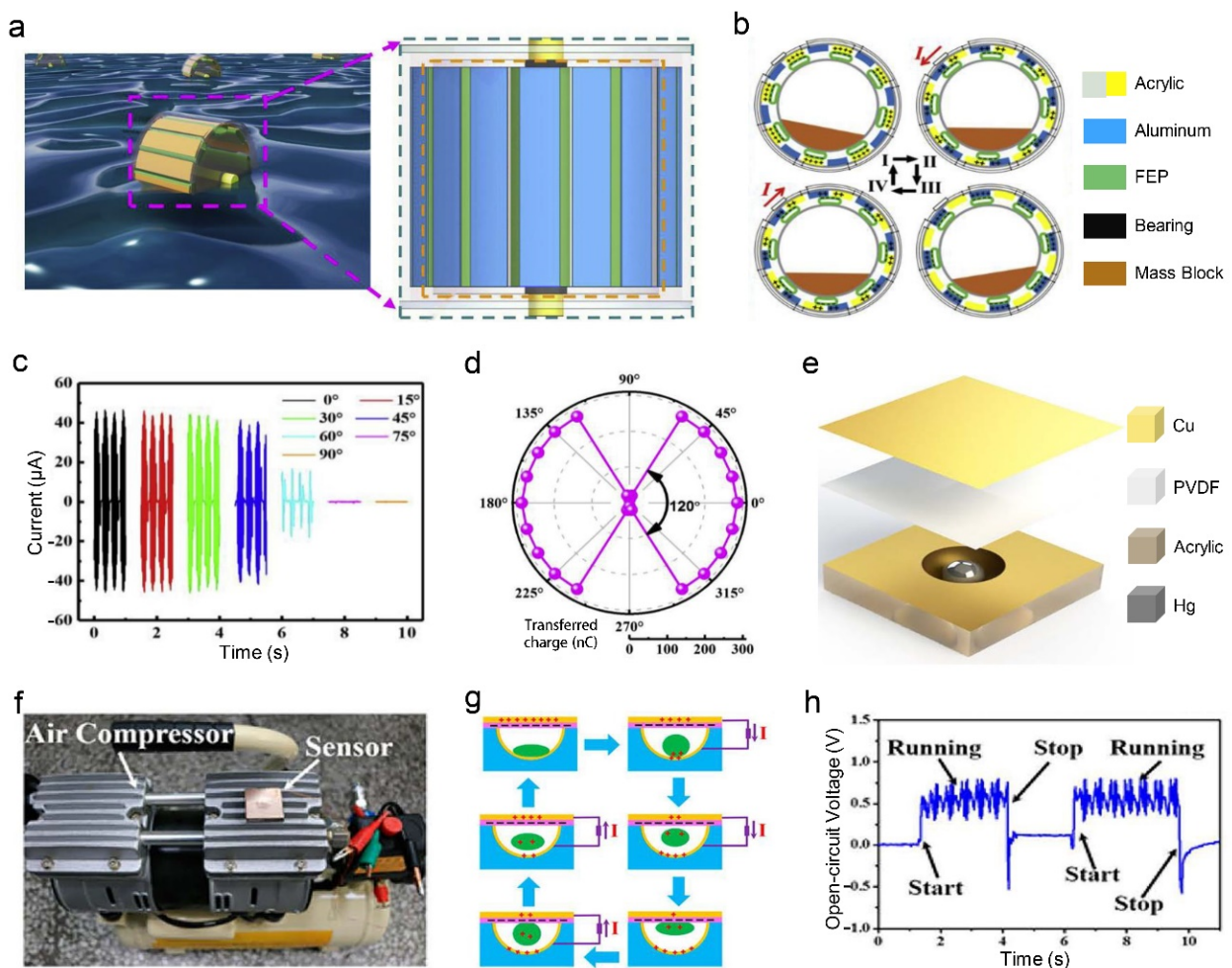


Figure 9. A curved surface contact vibration sensor: Part Two. (a) Schematic structure of the CP-TENG. (b) Working principle of the CP-TENG. (c) The short-circuit current of the CP-TENG at different angles. (d) Transferred charge of the CP-TENG at different excitation direction. Reproduced with permission [150]. Copyright 2020, Elsevier. (e) Structure design of the self-powered LM-TENG. (f) Demonstration of the LM-TENG fixed onto air compressor for vibration monitoring. (g) Working principle of the LM-TENG. (h) Open-circuit voltage of the LM-TENG during the start–stop process of the air compressor. Reproduced with permission [151]. Copyright 2017, American Chemical Society.

In summary, the application of TENG-based non-harmonic vibration sensor can sense vibration signals in the field of ship and ocean engineering and has achieved some research results. To achieve continuous monitoring of ship equipment and marine environment, this TENG-based non-harmonic vibration sensor should be stable and synchronous. The non-harmonic vibration does not rely on elastic bodies such as springs to achieve contact and separation of triboelectric materials, but on forced vibration at work to generate electrical signals that may not be synchronized with the vibration of the measured object. Therefore, future research can focus on how to synchronize the vibration state of the measured object with the sensing signal by means of data processing or system parameter adjustment. In addition, the intensity of the output signal is also very crucial for non-harmonic vibration sensors. The output signal of particle or powder contact vibration sensor is relatively weak, and the sensing signal will be very unclear in the case of large noise. Therefore, the next research direction should be how to increase the effective contact area between triboelectric materials through novel structural design to enhance the strength of the output vibration sensing signal.

4. Concluding Remarks and Future Perspectives

As the world marches into the era of Internet of Things, vibration sensors play an increasingly important role in the field of ship and ocean engineering and powering these distributed vibration sensors in the marine network is beyond the capability of traditional central power supply systems. It is time to develop a pervasive energy solution for smart and versatile sensors in the marine Internet of Things. Since the invention of the TENG in 2012, it has undergone tremendous development in sensing the vibration amplitude, direction, frequency, velocity, and acceleration in various forms. In this review article, the latest achievements of TENGs for sensing the vibration information in the field of ship and ocean engineering were systematically summarized, as shown in Table 1. With the emergence of new materials and new structures, to meet various application scenarios, different forms of marine TENG-based vibration sensors were developed and achieved more accurate vibration signal perception. For future field development, research directions can be implemented in the following aspects (Figure 10):

Table 1. A summary of structure characteristic and sensing property of various TENG-based vibration sensor.

Sensor Type	Structure Characteristic	Triboelectric Materials	Acceleration (m/s ²)	Amplitude (mm)	Velocity (m/s)	Frequency (Hz)	Sensitivity	Durability	Ref.
Harmonic vibration	Spring-assisted	Silicone rubber and carbon nanofiber	0~23	/	/	0~30	/	30,000	[95]
	Spring-assisted	PTFE and Cu	/	0.7~5	/	5~50	/	500,000	[109]
	Spring-based	Kapton and Al	1.07~1.25	/	/	/	/	/	[102]
	Spring-based	PMMA and Ag	/	1~6	0.6~1.1	30~60	/	/	[101]
	Spring-based	FE and TEL	/	0~40	/	0.5~2	/	10,000	[90]
	Elastomer-based	FEP-Al	/	/	/	1~22	/	200,000	[121]
	Elastomer-based	Silk-fibroin and PET	1~11	/	/	/	20.4 V/(m/s ²)	108,000	[106]
Non-harmonic vibration	Point contact	PTTEE and Ag	/	/	/	3~133 K	0.22 V/m/s	/	[127]
	Point contact	Ni and sugar	/	50~100	/	2.5~5.0	/	2000	[128]
	Curve contact	Cu and Hg and PVDF	0~60	/	/	/	0.26 V s/m ²	200,000	[151]
	Curve contact	PTFE and Cu	/	1~4.5	/	10~60	/	2000	[94]
	Curve contact	PP and SiO ₂	/	60~180	0~10	0.7~1.2	/	/	[149]
	Planar contact	Polyamide and Silicone	0~30	0~7.5	/	/	/	6000	[135]
	Planar contact	PVC and nylon	/	40~120	/	0.5~2.5	/	1500	[143]
	Planar contact	Silicone rubber and Aluminum	0.5~319.8	0.5~9	/	5~90	94.95 W/m ³	/	[142]

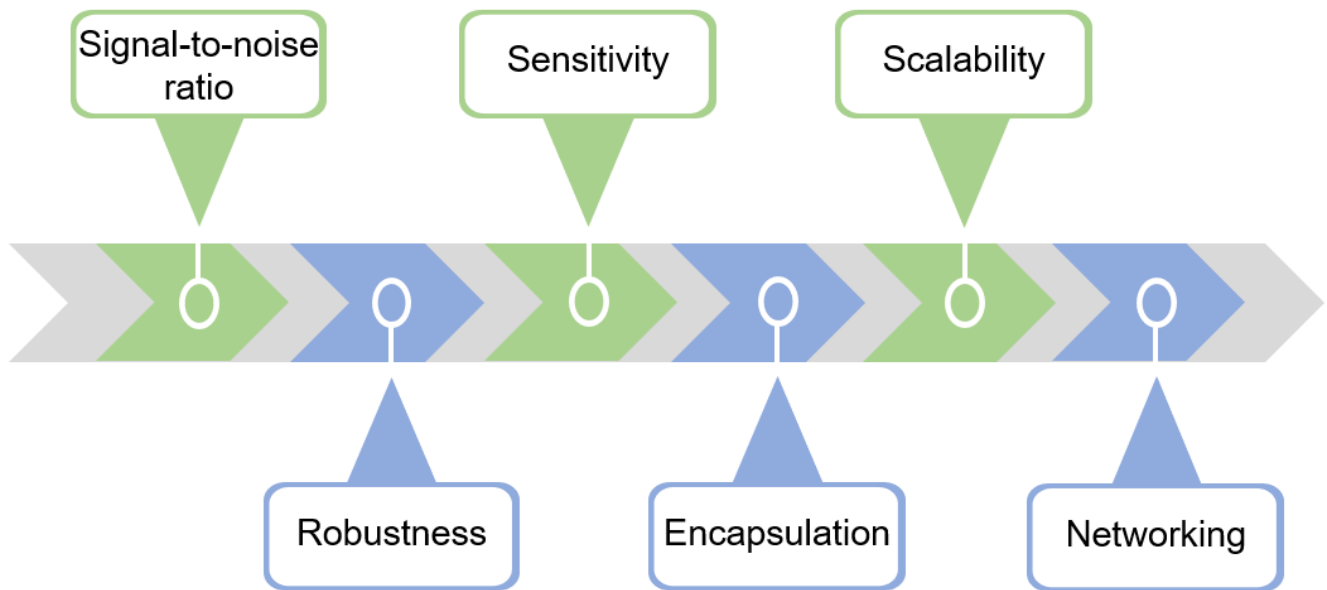


Figure 10. Perspectives of a TENG-based marine vibration sensor.

Signal-to-noise ratio refers to the ratio of normal vibration signal intensity to noise intensity. When the signal-to-noise ratio is low, such as triboelectric nanogenerator, the output signal is relatively weak, and the noise is easy to drown the normal signal, so it cannot be used to detect the vibration signal. Therefore, it is greatly significant to improve the signal-to-noise ratio of vibration signal. To our best knowledge, there are two ways to help solve this problem. (1) *Use the new digital filtering technology to filter out the noise interference.* The time-domain method of digital filtering is a method of filtering discrete vibration data signals by substituting them into difference equations. (2) *Improve the output signal intensity of the triboelectric nanogenerator.* As we all know, when the output signal intensity is relatively large, the signal-to-noise ratio will be relatively large. Physical structure modification [153], chemical methods [154] and bioengineering techniques [155] can be employed to enhance the output signal intensity of the triboelectric nanogenerator, thus improving the vibration signal-to-noise ratio.

Most of the existing micro/nano structures on the surfaces of triboelectric materials are not strong enough after long periods of operation, especially in lateral sliding mode. For example, nanostructures obtained by etching method are relatively easy to damage triboelectric materials, while those obtained by coating or electrospinning are easy to fall off. Therefore, it is necessary to study new technologies to improve the robustness and stability of triboelectric materials. One of the most effective approaches is to develop new triboelectric materials with the appropriate modulus, hardness and elasticity, since almost all triboelectric materials undergo continuous working cycle under elastic conditions. Another effective approach is to explore new surface treatment techniques. The use of the latest surface treatment technology ensures that the nanostructures on the surface of the triboelectric material are robust enough to remain stable after undergoing periodic mechanical stimulation.

Sensitivity is one of the most important parameters of vibration sensor, which refers to the response degree of a method to the change of unit quantity of substance to be measured. Increasing the sensitivity requires increasing the amplitude of the applied pulse or selecting more electro-sensitive triboelectric layer materials with higher charge density. Extending the detection range to a wider range is also important to improve sensitivity. According to the principle of TENG, the maximum and minimum values of sensor detection range are determined by the maximum and minimum output signals of TENG. Since the amount of initial charge affects the change in response, and the strength of contact or friction is critical

to the initial value of charge, so increasing the initial charge or friction strength will help raise the upper limit. Therefore, electro-sensitive and high charge density triboelectric layer materials can be selected to improve the initial charge increase, which can help improve the sensitivity [156]. In addition, micro/nano structures can also be used to increase the contact area of triboelectric materials and improve the sensitivity of vibration sensor.

Environmental factors such as temperature, humidity and salinity in the ocean and ships can negatively affect the accuracy and stability of TENG-based marine vibration sensors. Therefore, it is very important to package them efficiently. To overcome this, the following three things should be finished. (1) *Mechanical stability of encapsulation materials*. Encapsulation materials are required to have a certain high temperature resistance and can effectively overcome the mechanical wear between the encapsulation material and the equipment in the working process. (2) *Waterproofing of encapsulation materials*. Pipe leakage is easy to occur in the engine room of ships, and the high humidity in the engine room may affect the charge transfer of TENG-based vibration sensor, which will affect its normal operation. Therefore, it is urgent to study waterproof and moisture-proof encapsulation materials to resist the threat brought by water and moisture [157,158]. (3) *Chemical stability of encapsulation materials*. Vibration sensors applied in the field of ship and ocean engineering will inevitably encounter seawater, which is highly corrosive and will corrode encapsulation materials, so corrosion-resistant encapsulation materials should be selected to ensure their chemical stability.

Most TENG structures discussed above are produced considering functionality rather than device productivity. However, in order to make vibration sensing technology widely used in the field of ships, it must be easy to manufacture in an industrial environment. Several studies have taken advantage of existing manufacturing methods based on traditional machines to address this problem. However, techniques that provide nanomaterials with nanoscale properties, such as photolithography and nano etching, are also expensive and difficult to replicate in large quantities. This requires more research to develop cheaper and more efficient manufacturing processes suitable for large-scale production, especially induced surface properties to improve the output performance of TENG [159–161]. Meanwhile, in order to maximize the commercial value of TENG as a marine vibration sensor, another factor that must be investigated is the selection and development of new and inexpensive triboelectric materials that are easy to process, all of which are expected to facilitate the widespread use of TENG-based marine vibration sensing technology in the future.

Along with the booming development of Internet of Things and 5G wireless network, marine self-powered sensor network technology based on TENG is an inevitable development trend. TENG-based self-powered vibration sensor is an important part of ship sensor network. If progress is to be made, three issues must be thoroughly addressed. (1) *Communication between node sensors*. The data interaction and sharing of node sensors in the network is very important for the long-term development of the network, because it can not only perceive each other's working status, but also carry out multiple TENG cooperative operations to improve the working efficiency. (2) *Reaction to the Internet*. If TENG is connected to the Internet, all its performance parameters will be collected and transmitted to the shore-based Internet terminal. Shore-based experts can not only monitor the operating status of the equipment in real time, but also adjust the employment of TENG-based vibration sensors on the network according to the actual requirements of the equipment condition monitoring [162]. (3) *Modularization*. If the TENG-based vibration sensor is designed to be modular, it can be replaced by plug and pull in order to facilitate the daily maintenance of the crew.

Author Contributions: Conceptualization, Y.Z.; investigation, Y.Z., M.S., W.X. and X.Z.; resources, Y.Z.; data curation, M.S., W.X. and X.Z.; writing—original draft preparation Y.Z.; writing—review and editing, M.S., T.D., P.S. and M.X.; supervision, T.D., P.S. and M.X.; project administration, M.X.; All authors have read and agreed to the published version of the manuscript.

Funding: The work was supported by the National Natural Science Foundation of China (Grant Nos. 52101400, 52101345), the Fundamental Research Funds for the Central Universities, China (Grant Nos. 3132022212), the Dalian Outstanding Young Scientific and Technological Talents Project (2021RJ11), Scientific Research Fund of the Educational Department of Liaoning Province (LJKZ0055).

Institutional Review Board Statement: Not applicable.

Informed Consent Statement: Not applicable.

Data Availability Statement: Not applicable. This is a review article; all data and derived data are from referred literatures.

Conflicts of Interest: The authors declare no conflict of interest.

References

1. Lin, B. Research on Data Release and Location Monitoring Technology of Sensor Network Based on Internet of Things. *J. Web Eng.* **2021**, *20*, 689–711. [[CrossRef](#)]
2. Yang, H.; Kumara, S.; Bukkapatnam, S.T.; Tsung, F. The internet of things for smart manufacturing: A review. *IISE Trans.* **2019**, *51*, 1190–1216. [[CrossRef](#)]
3. Wang, Z.L. Entropy theory of distributed energy for internet of things. *Nano Energy* **2019**, *58*, 669–672. [[CrossRef](#)]
4. Choi, K.W.; Ginting, L.; Aziz, A.A.; Setiawan, D.; Park, J.H.; Hwang, S.I.; Kang, D.S.; Chung, M.Y.; Kim, D.I. Toward Realization of Long-Range Wireless-Powered Sensor Networks. *IEEE Wirel. Commun.* **2019**, *26*, 184–192. [[CrossRef](#)]
5. Zhou, Z.; Li, X.; Wu, Y.; Zhang, H.; Lin, Z.; Meng, K.; Lin, Z.; He, Q.; Sun, C.; Yang, J.; et al. Wireless self-powered sensor networks driven by triboelectric nanogenerator for in-situ real time survey of environmental monitoring. *Nano Energy* **2018**, *53*, 501–507. [[CrossRef](#)]
6. Jin, L.; Zhang, B.B.; Zhang, L.; Yang, W.Q. Nanogenerator as new energy technology for self-powered intelligent transportation system. *Nano Energy* **2019**, *66*, 104086. [[CrossRef](#)]
7. Askari, H.; Khajepour, A.; Khamesee, M.B.; Wang, Z.L. Embedded self-powered sensing systems for smart vehicles and intelligent transportation. *Nano Energy* **2019**, *66*, 104103. [[CrossRef](#)]
8. Xue, J.; Chen, Z.; Papadimitriou, E.; Wu, C.; Van Gelder, P.H.A.J.M. Influence of environmental factors on human-like decision-making for intelligent ship. *Ocean Eng.* **2019**, *186*, 106060. [[CrossRef](#)]
9. Li, H.; Iop. Research on Digital, Networked and Intelligent Manufacturing of Modern Ship. In Proceedings of the 3rd International Conference on Computer Information Science and Application Technology (CISAT), Dali, China, 17–19 July 2020.
10. Chi, X.; Liu, X. Design of Ship Intelligent Collision Prevention System Based on Computer Vision. *J. Coast. Res.* **2019**, *97*, 242–247. [[CrossRef](#)]
11. Cheng, R.; Wang, S.; Sun, L.; Gao, Y. A Study of the Marine Environment Monitoring Technology. *J. Coast. Res.* **2020**, *107*, 189–192. [[CrossRef](#)]
12. Xu, G.; Shen, W.; Wang, X.; IEEE. Marine Environment Monitoring Using Wireless Sensor Networks: A Systematic Review. In Proceedings of the IEEE International Conference on Systems, Man, and Cybernetics (SMC), San Diego, CA, USA, 5–8 October 2014.
13. Xu, G.; Shen, W.; Wang, X. Applications of Wireless Sensor Networks in Marine Environment Monitoring: A Survey. *Sensors* **2014**, *14*, 16932–16954. [[CrossRef](#)] [[PubMed](#)]
14. Chen, Y.; Ma, Q.; Liu, C.; Shu, Q. Research on marine environment monitoring based on Internet of things. *Desalin. Water Treat.* **2021**, *219*, 71–76. [[CrossRef](#)]
15. Chi, H.; Du, Y.; Brett, P.M. Design of a Marine Environment Monitoring System Based on the Internet of Things. *J. Coast. Res.* **2020**, *110*, 256–260. [[CrossRef](#)]
16. Zhang, H. Application of Wireless Sensor Network Based on ZigBee Technology in Marine Ecological Environment Monitoring. *J. Coast. Res.* **2020**, *110*, 54–56. [[CrossRef](#)]
17. Cho, J.-H. The Design and Development of Marine IT sensor Improving the Jitter Characteristic. *J. Korean Inst. Illum. Electr. Install. Eng.* **2020**, *34*, 55–60.
18. Garcia, E.; Quiles, E.; Correcher, A.; Morant, F. Sensor Buoy System for Monitoring Renewable Marine Energy Resources. *Sensors* **2018**, *18*, 945. [[CrossRef](#)]
19. Jiang, Y.; Dou, J.; Guo, Z.; Hu, K. Research of marine sensor web based on SOA and EDA. *J. Ocean Univ. China* **2015**, *14*, 261–268. [[CrossRef](#)]
20. Li, H.; Yu, H.; Yu, W.; Huang, S.; Liao, J.; Yan, J.; Chen, C.-C. Features of Vibration of Ship Generator Caused by Coupling Effect of Load Fluctuation. *Sens. Mater.* **2021**, *33*, 681–691. [[CrossRef](#)]
21. Zhuang, L. Design of Vibration Signal Data Acquisition System for Ship Mechanical and Electrical Equipment. *J. Coast. Res.* **2019**, *97*, 254–260. [[CrossRef](#)]
22. Xiong, X.-Y.; Wei, F.; Li, J.-W.; Han, M.; Guan, D.-H.; IEEE. Vibration Monitoring System of Ships Using Wireless Sensor Networks. In Proceedings of the 11th IEEE International Conference on Mechatronics and Automation (ICMA), Tianjin, China, 3–6 August 2014.

23. Ramilli, R.; Crescentini, M.; Traverso, P.A.; IEEE. Sensors for Next-Generation Smart Batteries in Automotive: A Review. In Proceedings of the 1st IEEE International Workshop on Metrology for Automotive (MetroAutomotive), Modena, Italy, 4–6 July 2021.
24. Lee, J.; Gye-choon, P. Battery Protection Method Using Gas Sensor Monitoring Device. *Trans. Korean Hydrog. New Energy Soc.* **2021**, *32*, 143–148. [[CrossRef](#)]
25. Lee, H.-J.; Kim, K.-T.; Park, J.-H.; Bere, G.; Ochoa, J.J.; Kim, T. Convolutional Neural Network-Based False Battery Data Detection and Classification for Battery Energy Storage Systems. *IEEE Trans. Energy Convers.* **2021**, *36*, 3108–3117. [[CrossRef](#)]
26. Li, H.; Yi, C.; Li, Y. Battery-Friendly Packet Transmission Algorithms for Wireless Sensor Networks. *IEEE Sens. J.* **2013**, *13*, 3548–3557. [[CrossRef](#)]
27. Li, T.; Guo, J.; Tan, Y.; Zhou, Z. Recent Advances and Tendency in Fiber Bragg Grating-Based Vibration Sensor: A Review. *IEEE Sens. J.* **2020**, *20*, 12074–12087. [[CrossRef](#)]
28. Li, P.; Wang, Y.; Wang, P.; Bai, Q.; Gao, Y.; Zhang, H.; Jin, B. Pulse Coding in Distributed Optical Fiber Vibration Sensor: A Review. *IEEE Sens. J.* **2021**, *21*, 22371–22387. [[CrossRef](#)]
29. Liu, X.; Jin, B.; Bai, Q.; Wang, Y.; Wang, D.; Wang, Y. Distributed Fiber-Optic Sensors for Vibration Detection. *Sensors* **2016**, *16*, 1164. [[CrossRef](#)] [[PubMed](#)]
30. Xu, S.; Xing, F.; Wang, R.; Li, W.; Wang, Y.; Wang, X. Vibration sensor for the health monitoring of the large rotating machinery: Review and outlook. *Sens. Rev.* **2018**, *38*, 44–64. [[CrossRef](#)]
31. Yang, J.S. A review of analyses related to vibrations of rotating piezoelectric bodies and gyroscopes. *IEEE Trans. Ultrason. Ferroelectr. Freq. Control* **2005**, *52*, 698–706. [[CrossRef](#)] [[PubMed](#)]
32. Devillez, A.; Dudzinski, D. Tool vibration detection with eddy current sensors in machining process and computation of stability lobes using fuzzy classifiers. *Mech. Syst. Signal Process.* **2007**, *21*, 441–456. [[CrossRef](#)]
33. Tian, G.Y.; Zhao, Z.X.; Baines, R.W. The research of inhomogeneity in eddy current sensors. *Sens. Actuators A Phys.* **1998**, *69*, 148–151. [[CrossRef](#)]
34. Xue, X.; Dong, Y.; Wu, X. Motion Induced Eddy Current Sensor for Non-Intrusive Vibration Measurement. *IEEE Sens. J.* **2020**, *20*, 735–744. [[CrossRef](#)]
35. Sun, X.; Chen, W.; Chen, W.; Qi, S.; Jiang, J.; Hu, C.; Tao, J. Damping vibration analysis of a dual-axis precision force sensor based on passive eddy current. *J. Phys. D-Appl. Phys.* **2020**, *53*, 255001. [[CrossRef](#)]
36. Hao, H.; Ji, Q. Vertical Vibration Conveyor Vibration Testing. In Proceedings of the International Conference on Frontiers of Manufacturing Science and Measuring Technology (ICFMM2011), Chongqing, China, 23–24 June 2011.
37. Li, Y.; Wang, Y.; Cao, Q.; Cao, J.a.; Qiao, D. A Self-Powered Vibration Sensor with Wide Bandwidth. *IEEE Trans. Ind. Electron.* **2020**, *67*, 560–568. [[CrossRef](#)]
38. Watanabe, Y.; Yahagi, T.; Abe, Y.; Murayama, H. Electromagnetic silicon MEMS resonator. *Electr. Eng. Jpn.* **2019**, *206*, 54–60. [[CrossRef](#)]
39. Qiu, J.; Wen, Y.; Li, P.; Liu, X.; Chen, H.; Yang, J. A resonant electromagnetic vibration energy harvester for intelligent wireless sensor systems. *J. Appl. Phys.* **2015**, *117*, 17B509. [[CrossRef](#)]
40. Ikegame, T.; Takagi, K.; Inoue, T.; Jikuya, I. Sensor-less parameter estimation of electromagnetic transducer and experimental verification. In Proceedings of the Conference on Active and Passive Smart Structures and Integrated Systems, San Diego, CA, USA, 9–12 March 2015.
41. Zhang, X.; Zhao, J.; Fu, X.; Lin, Y.; Qi, Y.; Zhou, H.; Zhang, C. Broadband vibration energy powered autonomous wireless frequency monitoring system based on triboelectric nanogenerators. *Nano Energy* **2022**, *98*, 107209. [[CrossRef](#)]
42. Li, M.; Zhang, Y.; Li, K.; Zhang, Y.; Xu, K.; Liu, X.; Zhong, S.; Cao, J. Self-powered wireless sensor system for water monitoring based on low-frequency electromagnetic-pendulum energy harvester. *Energy* **2022**, *251*, 123883. [[CrossRef](#)]
43. Huang, Y.; Zhao, C.; Tang, B.; Fu, H. Beacon Synchronization-Based Multi-Channel with Dynamic Time Slot Assignment Method of WSNs for Mechanical Vibration Monitoring. *IEEE Sens. J.* **2022**, *22*, 13659–13667. [[CrossRef](#)]
44. Zhan, Y.; Li, X.; Chang, L.; Zang, Y.; IEEE. Application of Wireless Sensor Network in Vibration Signal Monitoring System. In Proceedings of the International Conference on Mechatronic Sciences, Electric Engineering and Computer (MEC), Shenyang, China, 20–22 December 2013.
45. Nguyen, K.-D.; Kim, J.-T.; Park, Y.-H. Long-Term Vibration Monitoring of Cable-Stayed Bridge Using Wireless Sensor Network. *Int. J. Distrib. Sens. Netw.* **2013**, *9*, 1–9. [[CrossRef](#)]
46. Xue, W.; Dong, X.; Li, X. Study on Machinery Vibration Data Acquisition Node Based on Wireless Sensor Network. In Proceedings of the 2nd International Conference on Frontiers of Manufacturing Science and Measuring Technology (ICFMM 2012), Xi'an, China, 12–13 June 2012.
47. Han, C.G.; Guo, Y.B.; Jiang, C. Application for Vibration Monitoring of Aspheric Surface Machining Based on Wireless Sensor Networks. In Proceedings of the 5th International Symposium on Advanced Optical Manufacturing and Testing Technologies-Large Mirrors and Telescopes, Dalian, China, 26–29 April 2010.
48. Zhou, Y.; Dong, L.; Zhang, C.; Wang, L.; Huang, Q. Rotational Speed Measurement Based on LC Wireless Sensors. *Sensors* **2021**, *21*, 8055. [[CrossRef](#)] [[PubMed](#)]
49. Hong, Y.; Jia, P.; Guan, X.; Xiong, J.; Liu, W.; Zhang, H.; Li, C. Wireless Passive High-Temperature Sensor Readout System for Rotational-Speed Measurement. *J. Sens.* **2021**, *2021*, 6656527. [[CrossRef](#)]

50. Jiang, C.; Jiang, R.; He, W.; He, J.; IEEE. Comparative Experiments of Optical Fiber Sensor and Piezoelectric Sensor based on Vibration Detection. In Proceedings of the 4th IEEE International Conference on Frontiers of Sensors Technologies (ICFST), Shanghai, China, 6–9 November 2020.
51. Bian, Y.; Zhang, Y.; Sun, K.; Jin, H.; Dai, L.; Shen, H. A biomimetic vibration sensor using a symmetric electrodes metal core piezoelectric fiber. *J. Intell. Mater. Syst. Struct.* **2018**, *29*, 1015–1024. [[CrossRef](#)]
52. Andreev, Y.S.; Isaev, R.M.; Lubiviy, A.V.; Iop. Improvement of piezoelectric vibration sensors' performance characteristics via optimization of details' functional surfaces roughness. In Proceedings of the International Conference on Information Technologies in Business and Industry, Tomsk, Russia, 17–20 January 2018.
53. Tao, K.; Yi, H.; Tang, L.; Wu, J.; Wang, P.; Wang, N.; Hu, L.; Fu, Y.; Miao, J.; Chang, H. Piezoelectric ZnO thin films for 2DOF MEMS vibrational energy harvesting. *Surf. Coat. Technol.* **2019**, *359*, 289–295. [[CrossRef](#)]
54. Wu, Y.; Qiu, J.; Zhou, S.; Ji, H.; Chen, Y.; Li, S. A piezoelectric spring pendulum oscillator used for multi-directional and ultra-low frequency vibration energy harvesting. *Appl. Energy* **2018**, *231*, 600–614. [[CrossRef](#)]
55. Yamashita, K.; Nishioka, T.; Nishiumi, T.; Noda, M. Vibration Modes of Piezoelectric Diaphragms for Ultrasonic Microsensors and Influence of Top Electrodes. *Procedia Eng.* **2016**, *168*, 844–847. [[CrossRef](#)]
56. Alghisi, D.; Dalola, S.; Ferrari, M.; Ferrari, V. Ball-impact Piezoelectric Converter for Multi-degree-of-freedom Energy Harvesting from Broadband Low-frequency Vibrations in Autonomous Sensors. *Procedia Eng.* **2014**, *87*, 1529–1532. [[CrossRef](#)]
57. Wang, Z.L. New wave power. *Nature* **2017**, *542*, 159–160. [[CrossRef](#)]
58. Wang, Z.L. Triboelectric nanogenerators as new energy technology and self-powered sensors-Principles, problems and perspectives. *Faraday Discuss.* **2014**, *176*, 447–458. [[CrossRef](#)]
59. Wang, Z.L. Triboelectric Nanogenerators as New Energy Technology for Self-Powered Systems and as Active Mechanical and Chemical Sensors. *ACS Nano* **2013**, *7*, 9533–9557. [[CrossRef](#)] [[PubMed](#)]
60. Wang, Z.L. Self-Powered Nanosensors and Nanosystems. *Adv. Mater.* **2012**, *24*, 280–285. [[CrossRef](#)]
61. Zhang, H.; Marty, F.; Xia, X.; Zi, Y.; Bourouina, T.; Galayko, D.; Basset, P. Employing a MEMS plasma switch for conditioning high-voltage kinetic energy harvesters. *Nat. Commun.* **2020**, *11*, 3221. [[CrossRef](#)] [[PubMed](#)]
62. Wang, J.Q.; Zi, Y.L.; Li, S.Y.; Chen, X.Y. High-voltage applications of the triboelectric nanogenerator-Opportunities brought by the unique energy technology. *MRS Energy Sustain.* **2020**, *6*, e17. [[CrossRef](#)]
63. Nie, J.H.; Chen, X.Y.; Wang, Z.L. Electrically Responsive Materials and Devices Directly Driven by the High Voltage of Triboelectric Nanogenerators. *Adv. Funct. Mater.* **2019**, *29*, 1806351. [[CrossRef](#)]
64. Chen, B.; Yang, N.N.; Jiang, Q.; Chen, W.S.; Yang, Y. Transparent triboelectric nanogenerator-induced high voltage pulsed electric field for a self-powered handheld printer. *Nano Energy* **2018**, *44*, 468–475. [[CrossRef](#)]
65. Sun, D.-J.; Song, W.-Z.; Li, C.-L.; Chen, T.; Zhang, D.-S.; Zhang, J.; Ramakrishna, S.; Long, Y.-Z. High-voltage direct current triboelectric nanogenerator based on charge pump and air ionization for electrospinning. *Nano Energy* **2022**, *101*, 107599. [[CrossRef](#)]
66. Lu, S.; Lei, W.; Gao, L.; Chen, X.; Tong, D.; Yuan, P.; Mu, X.; Yu, H. Regulating the high-voltage and high-impedance characteristics of triboelectric nanogenerator toward practical self-powered sensors. *Nano Energy* **2021**, *87*, 106137. [[CrossRef](#)]
67. Li, Q.; Liu, W.; Yang, H.; He, W.; Long, L.; Wu, M.; Zhang, X.; Xi, Y.; Hu, C.; Wang, Z.L. Ultra-stability high-voltage triboelectric nanogenerator designed by ternary dielectric triboelectrification with partial soft-contact and non-contact mode. *Nano Energy* **2021**, *90*, 106585. [[CrossRef](#)]
68. Wang, X.; Chen, X.; Iwamoto, M. Recent progress in the development of portable high voltage source based on triboelectric nanogenerator. *Smart Mater. Med.* **2020**, *1*, 66–76. [[CrossRef](#)]
69. Zhao, C.; Liu, D.; Wang, Y.; Hu, Z.; Zhang, Q.; Zhang, Z.; Wang, H.; Du, T.; Zou, Y.; Yuan, H.; et al. Highly-stretchable rope-like triboelectric nanogenerator for self-powered monitoring in marine structures. *Nano Energy* **2022**, *94*, 106926. [[CrossRef](#)]
70. Zhao, T.; Xu, M.; Xiao, X.; Ma, Y.; Li, Z.; Wang, Z.L. Recent progress in blue energy harvesting for powering distributed sensors in ocean. *Nano Energy* **2021**, *88*, 106199. [[CrossRef](#)]
71. Xu, P.; Wang, X.; Wang, S.; Chen, T.; Liu, J.; Zheng, J.; Li, W.; Xu, M.; Tao, J.; Xie, G. A Triboelectric-Based Artificial Whisker for Reactive Obstacle Avoidance and Local Mapping. *Research* **2021**, *2021*, 9864967. [[CrossRef](#)]
72. Wang, Y.; Liu, D.; Hu, Z.; Chen, T.; Zhang, Z.; Wang, H.; Du, T.; Zhang, S.L.; Zhao, Z.; Zhou, T.; et al. A Triboelectric-Nanogenerator-Based Gas-Solid Two-Phase Flow Sensor for Pneumatic Conveying System Detecting. *Adv. Mater. Technol.* **2021**, *6*, 2001270. [[CrossRef](#)]
73. Wang, S.; Wang, Y.; Liu, D.; Zhang, Z.; Li, W.; Liu, C.; Du, T.; Xiao, X.; Song, L.; Pang, H.; et al. A robust and self-powered tilt sensor based on annular liquid-solid interfacing triboelectric nanogenerator for ship attitude sensing. *Sens. Actuators A-Phys.* **2021**, *317*, 112459. [[CrossRef](#)]
74. Phan, T.K.; Wang, S.; Wang, Y.; Wang, H.; Xiao, X.; Pan, X.X.; Xu, M.Y.; Mi, J.C. A Self-Powered and Low Pressure Loss Gas Flowmeter Based on Fluid-Elastic Flutter Driven Triboelectric Nanogenerator. *Sensors* **2020**, *20*, 729. [[CrossRef](#)] [[PubMed](#)]
75. Zhang, X.Q.; Yu, M.; Ma, Z.R.; Ouyang, H.; Zou, Y.; Zhang, S.L.; Niu, H.K.; Pan, X.X.; Xu, M.Y.; Li, Z.; et al. Self-Powered Distributed Water Level Sensors Based on Liquid-Solid Triboelectric Nanogenerators for Ship Draft Detecting. *Adv. Funct. Mater.* **2019**, *29*, 1900327. [[CrossRef](#)]
76. Xu, M.Y.; Wang, S.; Zhang, S.L.; Ding, W.B.; Kien, P.T.; Wang, C.; Li, Z.; Pan, X.X.; Wang, Z.L. A highly-sensitive wave sensor based on liquid-solid interfacing triboelectric nanogenerator for smart marine equipment. *Nano Energy* **2019**, *57*, 574–580. [[CrossRef](#)]

77. Zou, Y.; Xu, J.; Fang, Y.; Zhao, X.; Zhou, Y.; Chen, J. A hand-driven portable triboelectric nanogenerator using whirligig spinning dynamics. *Nano Energy* **2021**, *83*, 105845. [[CrossRef](#)]
78. Fang, Y.; Zou, Y.; Xu, J.; Chen, G.; Zhou, Y.; Deng, W.; Zhao, X.; Roustaei, M.; Hsiai, T.K.; Chen, J. Ambulatory Cardiovascular Monitoring Via a Machine-Learning-Assisted Textile Triboelectric Sensor. *Adv. Mater.* **2021**, *33*, e2104178. [[CrossRef](#)] [[PubMed](#)]
79. Wu, J.; Zheng, Y.; Li, X. Recent Progress in Self-Powered Sensors Based on Triboelectric Nanogenerators. *Sensors* **2021**, *21*, 7129. [[CrossRef](#)] [[PubMed](#)]
80. Park, J.Y.; Salauddin, M.; Rasel, M.S. Nanogenerator for scavenging low frequency vibrations. *J. Micromech. Microeng.* **2019**, *29*, 053001. [[CrossRef](#)]
81. Mohanty, A.; Parida, S.; Behera, R.K.; Roy, T. Vibration energy harvesting: A review. *J. Adv. Dielectr.* **2019**, *9*, 1930001. [[CrossRef](#)]
82. Dong, L.; Clossio, A.B.; Jin, C.; Tras, I.; Chen, Z.; Zhang, J.X. Vibration-Energy-Harvesting System: Transduction Mechanisms, Frequency Tuning Techniques, and Biomechanical Applications. *Adv. Mater. Technol.* **2019**, *4*, 1900177. [[CrossRef](#)] [[PubMed](#)]
83. Chen, J.; Wang, Z.L. Reviving Vibration Energy Harvesting and Self-Powered Sensing by a Triboelectric Nanogenerator. *Joule* **2017**, *1*, 480–521. [[CrossRef](#)]
84. Wang, Y.; Liu, X.; Chen, T.; Wang, H.; Zhu, C.; Yu, H.; Song, L.; Pan, X.; Mi, J.; Lee, C.; et al. An underwater flag-like triboelectric nanogenerator for harvesting ocean current energy under extremely low velocity condition. *Nano Energy* **2021**, *90*, 106503. [[CrossRef](#)]
85. Huang, C.; Li, Q.; Li, J.; Guo, H.; Hao, W.; Sheng, K.; An, Y.; Chen, J.; Zhang, X.; Xu, M. Research on dynamics of bouncing ball in triboelectric nanogenerator. *J. Micromech. Microeng.* **2021**, *31*, 085002. [[CrossRef](#)]
86. Wang, Y.; Yang, E.; Chen, T.; Wang, J.; Hu, Z.; Mi, J.; Pan, X.; Xu, M. A novel humidity resisting and wind direction adapting flag-type triboelectric nanogenerator for wind energy harvesting and speed sensing. *Nano Energy* **2020**, *78*, 105279. [[CrossRef](#)]
87. Xu, M.Y.; Wang, Y.C.; Zhang, S.L.; Ding, W.B.; Cheng, J.; He, X.; Zhang, P.; Wang, Z.J.; Pan, X.X.; Wang, Z.L. An aeroelastic flutter based triboelectric nanogenerator as a self-powered active wind speed sensor in harsh environment. *Extrem. Mech. Lett.* **2017**, *15*, 122–129. [[CrossRef](#)]
88. Zhao, H.F.; Xiao, X.; Xu, P.; Zhao, T.C.; Song, L.G.; Pan, X.X.; Mi, J.C.; Xu, M.Y.; Wang, Z.L. Dual-Tube Helmholtz Resonator-Based Triboelectric Nanogenerator for Highly Efficient Harvesting of Acoustic Energy. *Adv. Energy Mater.* **2019**, *9*, 1902824. [[CrossRef](#)]
89. Zou, Y.; Sun, M.; Yan, F.; Du, T.; Xi, Z.; Li, F.; Zhu, C.; Wang, H.; Zhao, J.; Sun, P.; et al. A High-Performance Flag-Type Triboelectric Nanogenerator for Scavenging Wind Energy toward Self-Powered IoTs. *Materials* **2022**, *15*, 3696. [[CrossRef](#)]
90. Li, S.X.; Liu, L.; Zhao, Z.H.; Zhou, L.L.; Yin, X.; Li, X.Y.; Gao, Y.K.; Zhang, C.G.; Zhang, Q.; Wang, J.; et al. A Fully Self-Powered Vibration Monitoring System Driven by Dual-Mode Triboelectric Nanogenerators. *ACS Nano* **2020**, *14*, 2475–2482. [[CrossRef](#)]
91. Xiao, T.X.; Liang, X.; Jiang, T.; Xu, L.; Shao, J.J.; Nie, J.H.; Bai, Y.; Zhong, W.; Wang, Z.L. Spherical Triboelectric Nanogenerators Based on Spring-Assisted Multilayered Structure for Efficient Water Wave Energy Harvesting. *Adv. Funct. Mater.* **2018**, *28*, 1802634. [[CrossRef](#)]
92. Zhang, H.; Yang, Y.; Su, Y.; Chen, J.; Adams, K.; Lee, S.; Hu, C.; Wang, Z.L. Triboelectric Nanogenerator for Harvesting Vibration Energy in Full Space and as Self-Powered Acceleration Sensor. *Adv. Funct. Mater.* **2014**, *24*, 1401–1407. [[CrossRef](#)]
93. Hu, Y.; Yang, J.; Jing, Q.; Niu, S.; Wu, W.; Wang, Z.L. Triboelectric Nanogenerator Built on Suspended 3D Spiral Structure as Vibration and Positioning Sensor and Wave Energy Harvester. *ACS Nano* **2013**, *7*, 10424–10432. [[CrossRef](#)] [[PubMed](#)]
94. Xiao, X.; Zhang, X.Q.; Wang, S.Y.; Ouyang, H.; Chen, P.F.; Song, L.G.; Yuan, H.C.; Ji, Y.L.; Wang, P.H.; Li, Z.; et al. Honeycomb Structure Inspired Triboelectric Nanogenerator for Highly Effective Vibration Energy Harvesting and Self-Powered Engine Condition Monitoring. *Adv. Energy Mater.* **2019**, *9*, 1902460. [[CrossRef](#)]
95. Xu, M.Y.; Wang, P.H.; Wang, Y.C.; Zhang, S.L.; Wang, A.C.; Zhang, C.L.; Wang, Z.J.; Pan, X.X.; Wang, Z.L. A Soft and Robust Spring Based Triboelectric Nanogenerator for Harvesting Arbitrary Directional Vibration Energy and Self-Powered Vibration Sensing. *Adv. Energy Mater.* **2018**, *8*, 1702432. [[CrossRef](#)]
96. Lian, Z.; Wang, Q.; Zhu, Q.; Zhao, C.; Zhao, Q.; Wang, Y.; Hu, Z.; Xu, R.; Lin, Y.; Chen, T.; et al. A Cantilever Beam-Based Triboelectric Nanogenerator as a Drill Pipe Transverse Vibration Energy Harvester Powering Intelligent Exploitation System. *Sensors* **2022**, *22*, 4287. [[CrossRef](#)]
97. Liu, J.; Huang, H.; Zhou, Q.; Wu, C. Self-Powered Downhole Drilling Tools Vibration Sensor Based on Triboelectric Nanogenerator. *IEEE Sens. J.* **2022**, *22*, 2250–2258. [[CrossRef](#)]
98. Chuan, W.; He, H.; Shuo, Y.; Chenxing, F. Research on the self-powered downhole vibration sensor based on triboelectric nanogenerator. *Proc. Inst. Mech. Eng. Part C J. Mech. Eng. Sci.* **2021**, *235*, 6427–6434. [[CrossRef](#)]
99. Wang, Y.N.; Gu, J.C.; Chen, C.M. The effect of harmonic torque to torsional vibration of induction machines. *J. Chin. Inst. Eng.* **1999**, *22*, 669–675. [[CrossRef](#)]
100. Li, X.; Shen, T. Harmonic vibration synchronization phenomenon analysis of dual excitation rotors nonlinear vibration system. *J. Vibroeng.* **2014**, *16*, 2843–2853.
101. Seolab, M.; Han, J.; Moon, D.; Yoon, K.; Hwang, C.; Meyyappan, M. All-printed triboelectric nanogenerator. *Nano Energy* **2018**, *44*, 82–88.
102. Zhao, X.J.; Wei, G.W.; Li, X.H.; Qin, Y.; Xu, D.D.; Tang, W.; Yin, H.J.; Wei, X.K.; Jia, L.M. Self-powered triboelectric nano vibration accelerometer based wireless sensor system for railway state health monitoring. *Nano Energy* **2017**, *34*, 549–555. [[CrossRef](#)]
103. Qi, Y.; Liu, G.; Gao, Y.; Bu, T.; Zhang, X.; Xu, C.; Lin, Y.; Zhang, C. Frequency Band Characteristics of a Triboelectric Nanogenerator and Ultra-Wide-Band Vibrational Energy Harvesting. *ACS Appl. Mater. Interfaces* **2021**, *13*, 26084–26092. [[CrossRef](#)] [[PubMed](#)]

104. Yu, H.; He, X.; Ding, W.B.; Hu, Y.S.; Yang, D.C.; Lu, S.; Wu, C.S.; Zou, H.Y.; Liu, R.Y.; Lu, C.H.; et al. A Self-Powered Dynamic Displacement Monitoring System Based on Triboelectric Accelerometer. *Adv. Energy Mater.* **2017**, *7*, 1700565. [[CrossRef](#)]
105. Liang, Q.; Zhanga, Z.; Yan, X.; Gu, Y.; Zhao, Y.; Zhang, G.; Lu, S.; Liao, Q.; Zhang, Y. Functional triboelectric generator as self-powered vibration sensor with contact mode and non-contact mode. *Nano Energy* **2015**, *14*, 209–216. [[CrossRef](#)]
106. Liu, C.R.; Wang, Y.S.; Zhang, N.; Yang, X.; Wang, Z.K.; Zhao, L.B.; Yang, W.H.; Dong, L.X.; Che, L.F.; Wang, G.F.; et al. A self-powered and high sensitivity acceleration sensor with V-Q-a model based on triboelectric nanogenerators (TENGs). *Nano Energy* **2020**, *67*, 104228. [[CrossRef](#)]
107. Gao, H.L.; Wang, Z.Y.; Cui, C.; Bao, J.Z.; Zhu, Y.B.; Xia, J.; Wen, S.M.; Wu, H.A.; Yu, S.H. A Highly Compressible and Stretchable Carbon Spring for Smart Vibration and Magnetism Sensors. *Adv. Mater.* **2021**, *33*, 2102724. [[CrossRef](#)]
108. Li, W.; Liu, Y.; Wang, S.; Li, W.; Liu, G.; Zhao, J.; Zhang, X.; Zhang, C. Vibrational Triboelectric Nanogenerator-based Multi-node Self-powered Sensor Network for Machine Fault Detection. *IEEE/ASME Trans. Mechatron.* **2020**, *25*, 2188–2196. [[CrossRef](#)]
109. Wu, H.; Wang, J.; Wu, Z.; Kang, S.; Wei, X.; Wang, H.; Luo, H.; Yang, L.; Liao, R.; Wang, Z.L. Multi-Parameter Optimized Triboelectric Nanogenerator Based Self-Powered Sensor Network for Broadband Aeolian Vibration Online-Monitoring of Transmission Lines. *Adv. Energy Mater.* **2022**, *12*, 2103654. [[CrossRef](#)]
110. He, J.; Fan, X.; Zhao, D.; Cui, M.; Han, B.; Hou, X.; Chou, X. A high-efficient triboelectric-electromagnetic hybrid nanogenerator for vibration energy harvesting and wireless monitoring. *Sci. China Inf. Sci.* **2021**, *65*, 142401. [[CrossRef](#)]
111. Chen, J.; Zhu, G.; Yang, W.Q.; Jing, Q.S.; Bai, P.; Yang, Y.; Hou, T.C.; Wang, Z.L. Harmonic-Resonator-Based Triboelectric Nanogenerator as a Sustainable Power Source and a Self-Powered Active Vibration Sensor. *Adv. Mater.* **2013**, *25*, 6094–6099. [[CrossRef](#)]
112. Wang, S.; Niu, S.; Yang, J.; Lin, L.; Wang, Z.L. Quantitative Measurements of Vibration Amplitude Using a Contact-Mode Freestanding Triboelectric Nanogenerator. *ACS Nano* **2014**, *8*, 12004–12013. [[CrossRef](#)] [[PubMed](#)]
113. Yang, W.Q.; Chen, J.; Jing, Q.S.; Yang, J.; Wen, X.N.; Su, Y.J.; Zhu, G.; Bai, P.; Wang, Z.L. 3D Stack Integrated Triboelectric Nanogenerator for Harvesting Vibration Energy. *Adv. Funct. Mater.* **2014**, *24*, 4090–4096. [[CrossRef](#)]
114. Wang, K.; Zhou, J.; Ouyang, H.; Chang, Y.; Xu, D. A dual quasi-zero-stiffness sliding-mode triboelectric nanogenerator for harvesting ultralow-low frequency vibration energy. *Mech. Syst. Signal Process.* **2021**, *151*, 107368. [[CrossRef](#)]
115. Quan, T.; Wu, Y.; Yang, Y. Hybrid electromagnetic-triboelectric nanogenerator for harvesting vibration energy. *Nano Res.* **2015**, *8*, 3272–3280. [[CrossRef](#)]
116. Pang, Y.K.; Li, X.H.; Chen, M.X.; Han, C.B.; Zhang, C.; Wang, Z.L. Triboelectric Nanogenerators as a Self-Powered 3D Acceleration Sensor. *ACS Appl. Mater. Interfaces* **2015**, *7*, 19076–19082. [[CrossRef](#)]
117. Wu, C.S.; Liu, R.Y.; Wang, J.; Zi, Y.L.; Lin, L.; Wang, Z.L. A spring-based resonance coupling for hugely enhancing the performance of triboelectric nanogenerators for harvesting low-frequency vibration energy. *Nano Energy* **2017**, *32*, 287–293. [[CrossRef](#)]
118. Yuan, Y.; Zhang, H.; Wang, J.; Xie, Y.; Khan, S.A.; Jin, L.; Yan, Z.; Huang, L.; Pan, T.; Yang, W.; et al. Hybrid nanogenerators for low frequency vibration energy harvesting and self-powered wireless locating. *Mater. Res. Express* **2018**, *5*, 015510. [[CrossRef](#)]
119. Wang, C.; Zhang, X.; Wu, J.; Yu, X.; Cheng, T.; Ma, H.; Wang, Z.L. Double-spring-piece structured triboelectric sensor for broadband vibration monitoring and warning. *Mech. Syst. Signal Process.* **2022**, *166*, 108429. [[CrossRef](#)]
120. Chen, Y.; Wang, Y.-C.; Zhang, Y.; Zou, H.; Lin, Z.; Zhang, G.; Zou, C.; Wang, Z.L. Elastic-Beam Triboelectric Nanogenerator for High-Performance Multifunctional Applications: Sensitive Scale, Acceleration/Force/Vibration Sensor, and Intelligent Keyboard. *Adv. Energy Mater.* **2018**, *8*, 1802159. [[CrossRef](#)]
121. Ren, Z.; Wu, L.; Zhang, J.; Wang, Y.; Wang, Y.; Li, Q.; Wang, F.; Liang, X.; Yang, R. Trapezoidal Cantilever-Structure Triboelectric Nanogenerator Integrated with a Power Management Module for Low-Frequency Vibration Energy Harvesting. *ACS Appl. Mater. Interfaces* **2022**, *14*, 5497–5505. [[CrossRef](#)]
122. Wu, C.; Huang, H.; Yang, S.; Wen, G. Pagoda-Shaped Triboelectric Nanogenerator with High Reliability for Harvesting Vibration Energy and Measuring Vibration Frequency in Downhole. *IEEE Sens. J.* **2020**, *20*, 13999–14006. [[CrossRef](#)]
123. Yang, W.Q.; Chen, J.; Zhu, G.; Wen, X.N.; Bai, P.; Su, Y.J.; Lin, Y.; Wang, Z.L. Harvesting vibration energy by a triple-cantilever based triboelectric nanogenerator. *Nano Res.* **2013**, *6*, 880–886. [[CrossRef](#)]
124. Nafari, A.; Sodano, H.A. Surface morphology effects in a vibration based triboelectric energy harvester. *Smart Mater. Struct.* **2018**, *27*, 015029. [[CrossRef](#)]
125. Wang, X.; Niu, S.; Yi, F.; Yin, Y.; Hao, C.; Dai, K.; Zhang, Y.; You, Z.; Wang, Z.L. Harvesting Ambient Vibration Energy over a Wide Frequency Range for Self-Powered Electronics. *ACS Nano* **2017**, *11*, 1728–1735. [[CrossRef](#)] [[PubMed](#)]
126. Zhang, H.; Su, X.; Quan, L.; Jiang, J.; Dong, B.; Wei, G. Sponge-Supported Triboelectric Nanogenerator for Energy Harvesting from Rail Vibration. *J. Energy Eng.* **2021**, *147*, 04021006. [[CrossRef](#)]
127. Lin, Z.; Sun, C.; Liu, W.; Fan, E.; Zhang, G.; Tan, X.; Shen, Z.; Qiu, J.; Yang, J. A self-powered and high-frequency vibration sensor with layer-powder-layer structure for structural health monitoring. *Nano Energy* **2021**, *90*, 106366. [[CrossRef](#)]
128. Lu, H.; Zhao, W.; Wang, Z.L.; Cao, X. Sugar-based triboelectric nanogenerators for effectively harvesting vibration energy and sugar quality assessment. *Nano Energy* **2021**, *88*, 106196. [[CrossRef](#)]
129. Vivekananthan, V.; Chandrasekhar, A.; Alluri, N.R.; Purusothaman, Y.; Khandelwal, G.; Pandey, R.; Kim, S.-J. Fe₂O₃ magnetic particles derived triboelectric-electromagnetic hybrid generator for zero-power consuming seismic detection. *Nano Energy* **2019**, *64*, 103926. [[CrossRef](#)]

130. Kim, D.; Jin, I.K.; Choi, Y.K. Ferromagnetic nanoparticle-embedded hybrid nanogenerator for harvesting omnidirectional vibration energy. *Nanoscale* **2018**, *10*, 12276–12283. [[CrossRef](#)]
131. Lai, S.-N.; Chang, C.-K.; Yang, C.-S.; Su, C.-W.; Leu, C.-M.; Chu, Y.-H.; Sha, P.-W.; Wu, J.M. Ultrasensitivity of self-powered wireless triboelectric vibration sensor for operating in underwater environment based on surface functionalization of rice husks. *Nano Energy* **2019**, *60*, 715–723. [[CrossRef](#)]
132. Zhang, H.; Wang, H.G.; Zhang, J.W.; Zhang, Z.C.; Yu, Y.; Luo, J.K.; Dong, S.R. A novel rhombic-shaped paper-based triboelectric nanogenerator for harvesting energy from environmental vibration. *Sens. Actuators A-Phys.* **2020**, *302*, 111806. [[CrossRef](#)]
133. Wang, L.; He, T.; Zhang, Z.; Zhao, L.; Lee, C.; Luo, G.; Mao, Q.; Yang, P.; Lin, Q.; Li, X.; et al. Self-sustained autonomous wireless sensing based on a hybridized TENG and PEG vibration mechanism. *Nano Energy* **2020**, *80*, 105555. [[CrossRef](#)]
134. Du, T.; Dong, F.; Xu, R.; Zou, Y.; Wang, H.; Jiang, X.; Xi, Z.; Yuan, H.; Zhang, Y.; Sun, P.; et al. A Drill Pipe-Embedded Vibration Energy Harvester and Self-Powered Sensor Based on Annular Type Triboelectric Nanogenerator for Measurement while Drilling System. *Adv. Mater. Technol.* **2022**, 2200003. [[CrossRef](#)]
135. Zhang, Z.; He, J.; Wen, T.; Zhai, C.; Han, J.; Mu, J.; Jia, W.; Zhang, B.; Zhang, W.; Chou, X.; et al. Magnetically levitated-triboelectric nanogenerator as a self-powered vibration monitoring sensor. *Nano Energy* **2017**, *33*, 88–97. [[CrossRef](#)]
136. Qu, Z.; Huang, M.; Dai, R.; An, Y.; Chen, C.; Nie, G.; Wang, X.; Zhang, Y.; Yin, W. Using non-contact eccentric nanogenerator to collect energy continuously under periodic vibration. *Nano Energy* **2021**, *87*, 106159. [[CrossRef](#)]
137. Park, M.; Cho, S.; Yun, Y.; La, M.; Park, S.J.; Choi, D. A highly sensitive magnetic configuration-based triboelectric nanogenerator for multidirectional vibration energy harvesting and self-powered environmental monitoring. *Int. J. Energy Res.* **2021**, *45*, 18262–18274. [[CrossRef](#)]
138. Hou, C.; Chen, T.; Li, Y.F.; Huang, M.J.; Shi, Q.F.; Liu, H.C.; Sun, L.N.; Lee, C. A rotational pendulum based electromagnetic/triboelectric hybrid-generator for ultra-low-frequency vibrations aiming at human motion and blue energy applications. *Nano Energy* **2019**, *63*, 103871. [[CrossRef](#)]
139. Chen, B.D.; Tang, W.; He, C.; Deng, C.R.; Yang, L.J.; Zhu, L.P.; Chen, J.; Shao, J.J.; Liu, L.; Wang, Z.L. Water wave energy harvesting and self-powered liquid-surface fluctuation sensing based on bionic-jellyfish triboelectric nanogenerator. *Mater. Today* **2018**, *21*, 88–97. [[CrossRef](#)]
140. Liang, Q.; Yan, X.; Liao, X.; Cao, S.; Lu, S.; Zheng, X.; Zhang, Y. Integrated active sensor system for real time vibration monitoring. *Sci. Rep.* **2015**, *5*, 16063. [[CrossRef](#)]
141. Chen, X.; Zeng, Q.; Shao, J.; Li, S.; Li, X.; Tian, H.; Liu, G.; Nie, B.; Luo, Y. Channel-Crack-Designed Suspended Sensing Membrane as a Fully Flexible Vibration Sensor with High Sensitivity and Dynamic Range. *ACS Appl. Mater. Interfaces* **2021**, *13*, 34637–34647. [[CrossRef](#)]
142. Du, T.; Ge, B.; Mtui, A.E.; Zhao, C.; Dong, F.; Zou, Y.; Wang, H.; Sun, P.; Xu, M. A Robust Silicone Rubber Strip-Based Triboelectric Nanogenerator for Vibration Energy Harvesting and Multi-Functional Self-Powered Sensing. *Nanomaterials* **2022**, *12*, 1248. [[CrossRef](#)] [[PubMed](#)]
143. Xia, K.; Fu, J.; Xu, Z. Multiple-Frequency High-Output Triboelectric Nanogenerator Based on a Water Balloon for All-Weather Water Wave Energy Harvesting. *Adv. Energy Mater.* **2020**, *10*, 2000426. [[CrossRef](#)]
144. Wang, Z.; Zhang, F.; Li, N.; Yao, T.; Lv, D.; Cao, G. Self-Powered Multifunctional Triboelectric Sensor Based on PTFE/PU for Linear, Rotary, and Vibration Motion Sensing. *Adv. Mater. Technol.* **2020**, *5*, 2000159. [[CrossRef](#)]
145. He, J.; Fan, X.; Mu, J.; Wang, C.; Qian, J.; Li, X.; Hou, X.; Geng, W.; Wang, X.; Chou, X. 3D full-space triboelectric-electromagnetic hybrid nanogenerator for high-efficient mechanical energy harvesting in vibration system. *Energy* **2020**, *194*, 116871. [[CrossRef](#)]
146. Pang, Y.K.; Chen, S.E.; Chu, Y.H.; Wang, Z.L.; Cao, C.Y. Matryoshka-inspired hierarchically structured triboelectric nanogenerators for wave energy harvesting. *Nano Energy* **2019**, *66*, 104131. [[CrossRef](#)]
147. Wu, C.; Huang, H.; Li, R.; Fan, C.X. Research on the Potential of Spherical Triboelectric Nanogenerator for Collecting Vibration Energy and Measuring Vibration. *Sensors* **2020**, *20*, 1063. [[CrossRef](#)]
148. Du, T.; Zuo, X.; Dong, F.; Li, S.; Mtui, A.E.; Zou, Y.; Zhang, P.; Zhao, J.; Zhang, Y.; Sun, P.; et al. A Self-Powered and Highly Accurate Vibration Sensor Based on Bouncing-Ball Triboelectric Nanogenerator for Intelligent Ship Machinery Monitoring. *Micromachines* **2021**, *12*, 218. [[CrossRef](#)]
149. Zhao, Z.; Zhang, Z.; Xu, L.; Gao, F.; Zhao, B.; Kang, Z.; Liao, Q.; Zhang, Y. Tumbler-shaped hybrid triboelectric nanogenerators for amphibious self-powered environmental monitoring. *Nano Energy* **2020**, *76*, 104960. [[CrossRef](#)]
150. Rui, P.S.; Zhang, W.; Zhong, Y.M.; Wei, X.X.; Guo, Y.C.; Shi, S.W.; Liao, Y.L.; Cheng, J.; Wang, P.H. High-performance cylindrical pendulum shaped triboelectric nanogenerators driven by water wave energy for full-automatic and self-powered wireless hydrological monitoring system. *Nano Energy* **2020**, *74*, 104937. [[CrossRef](#)]
151. Zhang, B.; Zhang, L.; Deng, W.; Jin, L.; Chun, F.; Pan, H.; Gu, B.; Zhang, H.; Lv, Z.; Yang, W.; et al. Self-Powered Acceleration Sensor Based on Liquid Metal Triboelectric Nanogenerator for Vibration Monitoring. *ACS Nano* **2017**, *11*, 7440–7446. [[CrossRef](#)]
152. Deng, H.; Zhao, Z.; Jiao, C.; Ye, J.; Zhao, S.; Ma, M.; Zhong, X. A Liquid-Metal-Based Freestanding Triboelectric Generator for Low-Frequency and Multidirectional Vibration. *Front. Mater.* **2021**, *8*, 692273. [[CrossRef](#)]
153. Zou, Y.; Xu, J.; Chen, K.; Chen, J. Advances in Nanostructures for High-Performance Triboelectric Nanogenerators. *Adv. Mater. Technol.* **2021**, *6*, 2000916. [[CrossRef](#)]
154. Xu, J.; Zou, Y.; Nashalian, A.; Chen, J. Leverage Surface Chemistry for High-Performance Triboelectric Nanogenerators. *Front. Chem.* **2020**, *8*, 57732. [[CrossRef](#)] [[PubMed](#)]

155. Zhou, Y.; Deng, W.; Xu, J.; Chen, J. Engineering Materials at the Nanoscale for Triboelectric Nanogenerators. *Cell Rep. Phys. Sci.* **2020**, *1*, 100142. [[CrossRef](#)]
156. Huang, C.; Chen, G.; Nashalian, A.; Chen, J. Advances in self-powered chemical sensing via a triboelectric nanogenerator. *Nanoscale* **2021**, *13*, 2065–2081. [[CrossRef](#)] [[PubMed](#)]
157. Xiong, J.Q.; Luo, H.S.; Gao, D.C.; Zhou, X.R.; Cui, P.; Thangavel, G.; Parida, K.; Lee, P.S. Self-restoring, waterproof, tunable microstructural shape memory triboelectric nanogenerator for self-powered water temperature sensor. *Nano Energy* **2019**, *61*, 584–593. [[CrossRef](#)]
158. Chen, X.X.; Miao, L.M.; Guo, H.; Chen, H.T.; Song, Y.; Su, Z.M.; Zhang, H.X. Waterproof and stretchable triboelectric nanogenerator for biomechanical energy harvesting and self-powered sensing. *Appl. Phys. Lett.* **2018**, *112*, 203902. [[CrossRef](#)]
159. Liu, C.; Li, J.; Che, L.; Chen, S.; Wang, Z.; Zhou, X. Toward large-scale fabrication of triboelectric nanogenerator (TENG) with silk-fibroin patches film via spray-coating process. *Nano Energy* **2017**, *41*, 359–366. [[CrossRef](#)]
160. Liu, G.; Gao, Y.; Xu, S.; Bu, T.; Xie, Y.; Xu, C.; Zhou, H.; Qi, Y.; Zhang, C. One-stop fabrication of triboelectric nanogenerator based on 3D printing. *Ecomat* **2021**, *3*, e12130. [[CrossRef](#)]
161. Lin, Z.M.; Yang, J.; Li, X.S.; Wu, Y.F.; Wei, W.; Liu, J.; Chen, J.; Yang, J. Large-Scale and Washable Smart Textiles Based on Triboelectric Nanogenerator Arrays for Self-Powered Sleeping Monitoring. *Adv. Funct. Mater.* **2018**, *28*, 1704112. [[CrossRef](#)]
162. Hung, L.-L. Intelligent Sensing for Internet of Things Systems. *J. Internet Technol.* **2022**, *23*, 185–191.